

Satellite derived national time series of giant kelp (*Macrocystis pyrifera*) abundance and key environmental drivers

New Zealand Aquatic Environment and Biodiversity Report No. 366

L.W. Tait

R. Pearson

A. Whiteside

F. Thoral

S. Mangan

ISSN 1179-6480 (online) ISBN 978-1-991407-08-5 (online)

October 2025



Te Kāwanatanga o AotearoaNew Zealand Government

Disclaimer

This document is published by Fisheries New Zealand, a business unit of the Ministry for Primary Industries (MPI). The information in this publication is not government policy. While every effort has been made to ensure the information is accurate, the Ministry for Primary Industries does not accept any responsibility or liability for error of fact, omission, interpretation, or opinion that may be present, nor for the consequence of any decisions based on this information. Any view or opinion expressed does not necessarily represent the view of Fisheries New Zealand or the Ministry for Primary Industries.

Enquiries should be directed to:

Fisheries Science Editor Fisheries New Zealand Ministry for Primary Industries PO Box 2526 Wellington 6140 NEW ZEALAND

Email: Fisheries-Science.Editor@mpi.govt.nz

Telephone: 0800 00 83 33

This publication is also available on the Ministry for Primary Industries websites at: http://www.mpi.govt.nz/news-and-resources/publications http://fs.fish.govt.nz go to Document library/Research reports

© Crown Copyright - Fisheries New Zealand

Please cite this report as:

Tait, L.W.; Pearson, R.; Whiteside, A; Thoral, F.; Mangan, S. (2025). Satellite derived national time series of giant kelp (*Macrocystis pyrifera*) abundance and key environmental drivers. *New Zealand Aquatic Environment and Biodiversity Report No. 366.* 50 p.

TABLE OF CONTENTS

EXECUTIVE SUMMARY		1
1	INTRODUCTION	2
	1.1 OVERVIEW	3
	1.2 OBJECTIVES	4
2	METHODS	4
	2.1 Quantifying kelp cover	4
	2.2 Sea surface temperature and light attenuation	6
	2.3 Data analysis	7
3	RESULTS	8
	3.1 National distribution and abundance of kelp	8
	Region 1: Wellington, Marlborough Sounds	10
	Region 2: Kaikōura and Canterbury	13
	Region 3: Chatham Island	18
	Region 4: Otago	19
	Region 5: Southland, Fiordland and Rakiura	21
	Region 6: Sub-Antarctic Islands	25
	3.2 Environmental drivers of kelp abundance	28
4	DISCUSSION	40
5	POTENTIAL RESEARCH	42
6	FULFILLMENT OF BROADER OUTCOMES	43
7	ACKNOWLEDGEMENTS	44
8	REFERENCES	44

PLAIN LANGUAGE SUMMARY

Giant kelp is one of the largest and fastest growing seaweeds in the world, it provides food and habitat for marine life, and engineers the physical environment around it. It is also a managed fishery in Aotearoa New Zealand. Because of its key role in supporting marine fisheries (particularly pāua, kina, kōura, and several key finfish) and the increasing interest in the commercial harvesting of seaweeds, we need a greater understanding of the current distribution of giant kelp.

Here we utilise satellite remote sensing to track the distribution of giant kelp across Aotearoa New Zealand over the last decade. Satellites provide a passive and free tool for monitoring the expanse of surface canopies. This is particularly relevant as kelp forest ecosystems are impacted by extreme events such as marine heatwaves and cyclones.

We show that satellite remote sensing of giant kelp can be used effectively to track the status and health of giant kelp which provides a powerful tool for identifying the drivers of change in kelp beds. By looking for relationships between key environmental parameters and kelp forest coverage, we found that national level declines in giant kelp beds are highly associated with periods of warmer oceanic conditions.

We provide a summary of regional trends of giant kelp coverage and assess the environmental factors that drive variation. This work is accompanied by a web interface that allows managers and stakeholders to view and assess satellite products and the outputs of our kelp cover estimates.

EXECUTIVE SUMMARY

Tait, L.W.¹; Pearson, R.; Whiteside, A.; Thoral, F.; Mangan, S. (2025). Satellite derived national time series of giant kelp (*Macrocystis pyrifera*) abundance and key environmental drivers. *New Zealand Aquatic Environment and Biodiversity Report No. 366.* 50 p.

Giant kelp (*Macrocystis pyrifera*) is an iconic habitat-forming species inhabiting shallow subtidal rocky reefs. It forms complex three-dimensional habitat for a wide range of invertebrates and finfish (e.g., pāua, kina, kōura, and rarī/butterfish/greenbone) many of which are commercially, recreationally, and/or culturally significant. *Macrocystis* is also a managed fishery and is included in New Zealand's Quota Management System (QMS), with a total allowable harvest of over 1500 tonnes.

Given its key role in supporting marine fisheries and the increasing interest in the commercial harvesting of seaweeds, an understanding of the distribution and health of giant kelp is increasingly required. Global patterns of kelp geographies have revealed a weak net loss of kelp, but at regional scales these habitats have been heavily impacted by diverse combinations of stressors such as altered nutrient regimes, overfishing at higher trophic levels, storms and waves, sedimentation, and heatwaves.

Despite the importance and vulnerability of giant kelp, there are no quantitative assessments of giant kelp distribution or abundance nationally. This report, as part of a wider programme, aims to, 1) develop an updatable layer of giant kelp distribution, and 2) aid in the analysis of climate impacts on giant kelp. Continuous satellite-based monitoring offers a cost-effective, and scalable approach to tracking kelp distribution, abundance, and condition, and can support fisheries and ecosystem management. Given the vast, remote, and variable nature of New Zealand's *Macrocystis* populations, satellite remote sensing provides an effective tool capable of delivering nationwide coverage.

Here we implement a satellite remote sensing framework to map and monitor giant kelp nationally. Regions with the most extensive kelp forests include the Otago Region (Waikouaiti-Oamaru), the Chatham Islands, Campbell Island, Auckland Island, Rakiura, and Akaroa. We identify generally consistent coverage of giant kelp through time, although locations varied greatly in their capacity for supporting giant kelp beds. However, we note several regions with negative trends, including:

- **Timaru** –a notable trend of decline through time. From 2015–2017 there was high coverage of giant kelp but this declined dramatically from 2018–2025.
- **Porirua** had a strong decline in kelp cover with increasing SST was evident and this region experienced temperatures above upper thresholds for *Macrocystis*.
- Wharanui-Kekerengu –timeseries showed declining kelp cover with increasing temperatures and this region is close to the upper end of the temperature threshold for *Macrocystis*.
- **Chathams** initially one of the regions with the greatest kelp cover, but from 2018–2025 there was a sustained decline in kelp cover.

We show that satellite remote sensing presents a cost-effective option for management purposes and provides decadal scale observations across broad biogeographic zones. We note that several large giant kelp beds have been identified by this work including beds near Mana Island and Kaikōura. Furthermore, we note significant negative trends in giant kelp cover associated with warmer oceanographic conditions, although many regions show rapid recovery following these events.

This research and the online tool we provide will be able to inform agencies from the Ministry of Primary Industries (Fisheries New Zealand) to local and regional councils about trends of macroalgal populations and allow the inference of broad ecological impacts of climatic events. Furthermore, few spatially explicit timeseries for kelp exist for the sub-Antarctic Islands. The research here shows that satellite remote sensing can be successfully applied to southernmost portion of New Zealand's EEZ and could inform the conservation of these ecologically significant islands.

-

¹ Earth Sciences New Zealand.

1 INTRODUCTION

Macrocystis pyrifera /giant kelp is an iconic and conspicuous, habitat-forming, foundation species inhabiting shallow subtidal rocky reefs along the southern coastline of Aotearoa New Zealand (hereafter New Zealand), with its northern range reaching approximately 41°S (Hay, 1990; Nelson, 2020). Characterised by extensive surface-floating canopies and high productivity, Macrocystis supports diverse biological communities and contributes to a wide range of amenity, ecological, economic and intrinsic values (Foster & Schiel 1985; Hepburn et al. 2007; Reed et al. 2016; Mabin et al. 2019; Tait 2019, Bennett et al. 2015; Eger et al. 2023; Hynes et al. 2021).

The complex three-dimensional structure of *Macrocystis* forests provide essential habitat for a wide range of invertebrates and finfish, many of which are commercially, recreationally, and/or culturally significant. Species such as pāua, kina, kōura/red rock lobster (*Jasus edwardsii*), and rarī/butterfish/greenbone (*Odax pullus*) rely on kelp forests for shelter, and also for settlement, and food throughout their life cycles. Beyond direct habitat provision, *Macrocystis* contributes substantially to coastal food webs through the production of suspended particulate organic matter, detritus, and epifaunal biomass (Schlieman et al. 2022; Wing & Jack 2012). These organic matter pathways support secondary consumers and suspension feeders, linking kelp forest health directly to the productivity of certain fisheries and to higher trophic levels (Jack & Wing 2011; Jack et al. 2009; Kolodzey et al. 2023; Wing et al. 2012). These ecosystem services are critical to the resilience and productivity of coastal fisheries and have been valued in the billions of dollars annually at regional and global scales (Vásquez et al. 2014, Eger et al. 2023).

Macrocystis is also a managed fishery in its own right and is included in New Zealand's Quota Management System (QMS), with a total allowable harvest of over 1500 tonnes. Commercial interest in giant kelp harvest, as well as a range of other species, extends beyond direct harvest for food and fertiliser (e.g., Schiel & Nelson 1990; White & White 2020), to the extraction of high-value biomolecules such as alginate, fucoidan, and phlorotannins, which have applications in pharmaceuticals, cosmetics, and nutraceuticals (Kim & Bhatnagar, 2011; Mak et al. 2013; Porse & Rudolph 2017).

Given its key role in supporting marine fisheries (particularly pāua, kina, kōura, and several key finfish) and the increasing interest in the commercial harvesting of seaweeds, an understanding of the distribution and health of giant kelp is required. Global patterns of kelp geographies have revealed a weak net loss of kelp (Krumhansl et al. 2016), but at regional scales these habitats have been heavily impacted by diverse combinations of stressors such as altered nutrient regimes (Connell et al. 2008; Mangialajo et al. 2008; Perkol-Finkel & Airoldi, 2010), overfishing at higher trophic levels (Tegner & Dayton 2000; Steneck et al. 2002; Shears et al. 2008; Ling et al. 2009), storms and waves (Seymour et al. 1989; Reed et al. 2011), sedimentation (Connell 2005; Gorgula & Connell, 2004; Foster & Schiel, 2010), and heatwaves (Gaitán-Espitia et al. 2014; Wernberg et al. 2016). These pressures can lead to persistent shifts in ecosystem states, such as dominance by turfing algae (Filbee-Dexter & Wernberg, 2018) or urchin barrens (Shears & Babcock 2002; Filbee-Dexter & Scheibling 2014).

Rising temperature is a particularly significant driver of kelp forest decline globally. This includes long-term warming trends, short-term temperature anomalies, and increasingly frequent, intense, and prolonged marine heatwaves (MHWs) (Frölicher et al. 2018; Hobday et al. 2018; Gupta et al. 2020). MHWs have been linked to kelp forest degradation in regions such as Tasmania (Oliver et al. 2018), Western Australia (Wernberg et al. 2013, 2016), North America (Arafeh-Dalmau et al. 2019; Rogers-Bennett & Catton, 2019) and Europe (Filbee-Dexter et al. 2020), and have, in extreme cases, caused range contractions and regional extinctions (Smale & Wernberg 2013; Wernberg et al. 2016; Straub et al. 2019; Smale, 2020). Temperature affects all aspects of biology, from subcellular biochemical reaction rates to reproductive success, evolutionary mutation rates and selection pressures (Hoegh-Guldberg & Bruno, 2010; Doney et al. 2011). While high temperatures can have predictable physiological effects on kelp tissue and population growth rates (Tait 2014; Mabin et al. 2019), broader ecological impacts on abundances, communities and ecosystem functioning are complicated by indirect effects, altered competitive hierarchies, the timing and magnitude of specific MHWs and the latitudinal distribution and thermal responses of individual kelp species (Doney et al. 2011; Wernberg et al. 2016;

Smale et al. 2019). For instance, kelp populations near their equatorward range limits tend to experience strong negative impacts from MHWs, while those near colder, poleward boundaries may show neutral or even positive responses (Wernberg et al. 2010, 2016; Reed et al. 2016; Arafeh-Dalmau et al. 2019; Cavanaugh et al. 2019). These spatially variable responses underscore the importance of understanding regional thermal tolerances and climate dynamics when assessing the resilience of kelp forests under future warming scenarios.

Another prevalent pressure both globally and in New Zealand is sedimentation and the resulting increase in water column turbidity, as they can significantly alter physical, biological and biogeochemical properties and processes. In New Zealand, these issues are particularly pronounced due to extensive land-based anthropogenic activities such as deforestation, agriculture, urbanisation, and coastal development, which intensify coastal erosion. Sedimentation can affect macroalgal distribution across both rocky and soft sediment habitats (Airoldi 2003), including within New Zealand (Morrison et al. 2009; Wing et al. 2022), by disrupting kelp settlement and attachment during microscopic stages and reducing spore survival through scouring and burial (Arakawa & Matsuike 1992; Chapman et al. 2002; Devinny & Volse 1978; Schiel et al. 2006). In adult kelps, sedimentation can lower productivity, hinder growth, and impair regeneration, ultimately influencing species composition and distribution (Alestra et al. 2014; Airoldi 2003).

Concurrent with sedimentation is increased water column turbidity from suspended particles, which can severely limit the energy available for photosynthetic carbon fixation (Gattuso et al. 2006). Given that macroalgae can contribute up to 90% of total carbon in coastal food webs (Gattuso et al. 2006), such reductions have direct implications for ecosystem functioning and carbon sequestration (Blain et al. 2021), and may also affect the resilience of kelp populations to other environmental (e.g., heat; Wernberg et al. 2016) and biological (e.g., urchins; Ling et al. 2015) stressors. While macroalgae can respond to fluctuations in light availability through mechanisms such as dynamic photoinhibition, pigment acclimation, and morphological adaptations that enhance light absorption efficiency (Blain et al. 2020; Colombo-Pallotta et al. 2006; Johansson & Snoeijs 2002), persistent light limitation can affect the density (Kirkman, 1989), biomass (Desmond et al. 2015), and depth distribution (Kautsky et al. 1986) of habitat-forming seaweeds.

Leveraging key datasets that provide evidence of the spatio-temporal variability of kelp and macroalgae may provide a novel and useful tool for improving our understanding of their distribution and extent. Passive remote sensing is now widely used (Bell et al. 2020; Huovinen et al. 2020; Mora-Soto et al. 2020; Hamilton et al. 2020) and typically relies on vegetation indices derived from near-infrared electromagnetic radiation to detect surface-floating macroalgal canopies. While this method provides direct measurements of visible canopy cover, it cannot detect subsurface kelp forests, limiting insights into the full population dynamics of *Macrocystis*. Nevertheless, surface canopy cover remains a valuable proxy for overall forest health, and remotely sensed time series data have proven effective in identifying kelp bed responses to multiple stressors (Cavanaugh et al. 2011). Continuous satellite-based monitoring offers a cost-effective, scalable, and timely approach to tracking kelp distribution, abundance, and condition, and can support more informed fisheries and ecosystem management. Given the vast, remote, and variable nature of New Zealand's *Macrocystis* populations, satellite remote sensing stands provides an immediately deployable tool capable of delivering nationwide coverage.

1.1 OVERVIEW

This report is part of a wider programme to quantify the role of macroalgae in key fisheries (particularly commercial fisheries) and understand the distribution of and impacts of climate change on giant kelp. This report is supported by a review on the importance of macroalgae to New Zealand's nearshore fisheries (Mangan et al. 2025). This report aims to, 1) develop an updatable layer of giant kelp distribution that can be maintained over time, and 2) aid in the analysis of climate impacts on giant kelp.

We use satellite remote sensing to detect and track kelp forests, particularly *Macrocystis pyrifera*, across its range in Aotearoa New Zealand. We present regional distributions and trends and assess the key

environmental drivers of change. A goal for this programme of work was to develop a publicly accessible interface that could be perpetually updated with estimates of kelp cover at a national scale. Alongside the results from this project NIWA have developed an automated online interface for plotting and visualising the abundance and distribution of *Macrocystis pyrifera*. This interface is intended to automatically update as new satellite imagery becomes available.

1.2 OBJECTIVES

The objectives of this report are:

- To deliver a time-series of the abundance and distribution of *Macrocystis pyrifera* across its entire range in Aotearoa (including offshore and sub-Antarctic islands).
- To identify and project how climate change may influence these trends and affect the abundance and distribution of *Macrocystis pyrifera*.

2 METHODS

We used the multispectral Sentinel-2 satellite constellation to detect and filter kelp from ocean pixels across Aotearoa New Zealand. We leveraged existing published algorithms for the detection and filtering of kelp (Cavanaugh et al. 2011, Bell et al. 2020; Mora-Soto et al. 2020, Tait et al. 2021) and developed additional steps and algorithms to further improve the robustness of kelp detections in the New Zealand wide context. These algorithms target canopies of aquatic vegetation (not restricted to *Macrocystis pyrifera*) close to, or at the surface of the ocean, and are unable to detect vegetation occluded by significant overlying water, giving a direct measurement of only the floating or exposed portion of macroalgal canopies.

2.1 Quantifying kelp cover

Surface canopies of *Macrocystis* were assessed using Sentinel-2 satellite imagery (resolution = 100 m²) between December 2015 (start date for Sentinel-2 satellite) and December 2024 (Copernicus Sentinel-2A data 2015–2024). In total, 25 focal regions spanning 10° of latitude across New Zealand's Exclusive Economic Zone (EEZ) were chosen, relating to key populations as determined by Hay (1990) (Figure 1). Within the focal regions polygons defining large areas of varying sizes were created to examine *Macrocystis* beds. Polygon size depended on how much is known about the distribution of kelp in the given region. Some regions have well known kelp beds that are discrete, while others have received limited attention and, therefore, have been encompassed by large polygons to examine the potential for unknown populations.

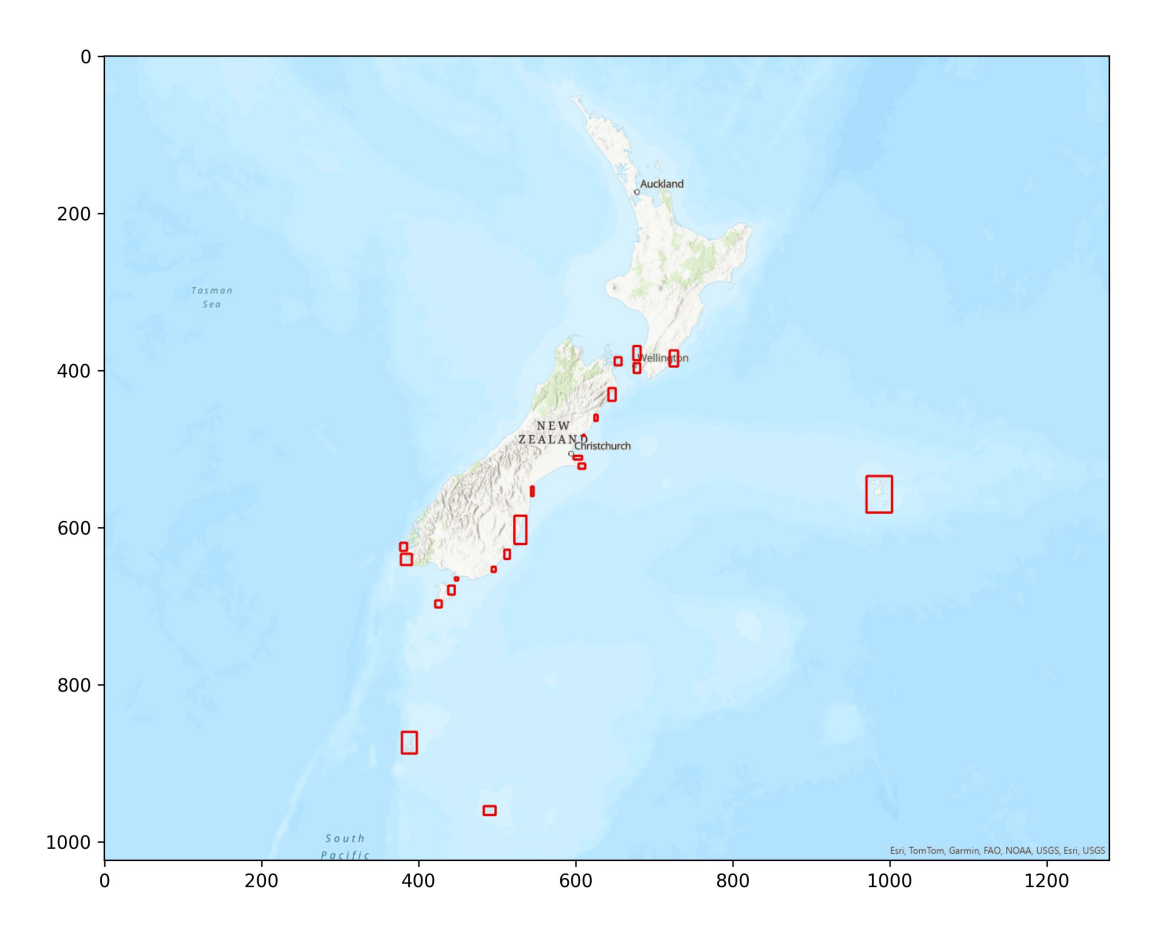


Figure 1: Distribution of sampling polygons across Aotearoa New Zealand and offshore Islands. Each polygon defines the region that Sentinel-2 satellite imagery was assessed across the full available record.

A two-pass algorithm utilising established multi-band indices was used to differentiate kelp from other features through a series of masking and filtering procedures. Specifically, the Normalised Difference Vegetation Index (NDVI) and the Normalised Difference Water Index (NDWI) were used. The algorithm steps include:

- Cloud-free images were selected by using the quality control bands (Sentinal-2 QA band 60). Only images with less than 5% cover over the coastal ocean region were selected.
- All mainland and offshore island pixels were removed by masking with the Land Information New Zealand NZ Coastlines and Islands Polygons (Topo 1:50k) layer.
- Filtering by NDVI to keep only pixels with a vegetation signal, and by the two different NDWI indices to keep only pixels without a strong water signal.
- Filtering with a much larger NDVI threshold and the same NDWI thresholds to detect dense kelp beds. Any dates where the kelp beds and dense kelp bed areas differ by more than 20 times are removed as this indicates that the thresholding approach is not suitable. These dates are removed from further analysis.
- Morphological filtering to keep only clusters of kelp with an area of at least 1000 m² or 10 connected pixels followed by buffering at 100 m (or 10 pixels) to define the region of interest over which to apply the second pass of the algorithm.

 Filtering by NDVI to keep only pixels with a vegetation signal, and by the two different NDWI indices to keep only pixels without a strong water signal within the restricted region of interest.

The bands B3 (559.8 nm) and B8 (832.8 nm) were used to calculate the first NDWI, bands B5 (704.1 nm) and B11 (1613.7 nm) were used to calculate the second NDWI, and B4 (664.6 nm), and B6 (740.5 nm) was used to calculate NDVI.

These procedures were used to detect kelp cover across the New Zealand region and for the timeseries available from the Sentinel-2 satellite constellation. Kelp within each of the areas of interest was quantified in two ways:

- 1. Total area covered by kelp for each individual satellite pass.
- 2. Proportion of the maximum kelp cover.

Maximum kelp cover was defined as the cumulative occupation of all pixels across the full timeseries. For example, every positive detection from 2015–2024 was combined into a single map of "maximum kelp cover". For each date for which appropriate imagery was available, maximum kelp cover was:

$$Proportional \ kelp \ cover = \frac{Kelp \ cover_t}{Maximum \ kelp \ cover_t}$$

Where *Maximum kelp cover* is the cumulative area covered by kelp at a site across the whole timeseries (m^2), and *Kelp cover*_t is the cover of kelp for each timestep (m^2).

Kelp detection results were previously tested against *in situ* subtidal densities of *Macrocystis* (Tait et al. 2021). Although the method does not provide a specific canopy area per pixel, instead assuming 100% canopy coverage within pixels, similar NDVI based vegetation detection methods have been shown to provide an effective proxy for kelp extent and abundance (Cavanaugh et al. 2010; Nijland et al. 2019). This provides a standardised method for identifying the presence and relative extent of kelp beds to identify spatio-temporal trends in relation to key environmental parameters (Butler et al. 2020).

The application of the kelp detection process was automated across the selected sites (Figure 1) and across the time range. Sentinel-2 data was accessed pragmatically in Python using the publicly available Microsoft Planetary Data Spatio Temporal Asset Catalog (STAC), which is a hosting of the underlying Copernicus dataset with support for spatial, temporal and cloud coverage queries. The New Zealand specific kelp detection algorithm was also developed in Python. The overall process can be run in one step across all sites and date ranges to produce date-by-date kelp detections of all suitable sites. These are then reviewed through a web-dashboard to ensure that there are no anomalous results. We detected 8 anomalous dates across 2600 dates across all sites. Anomalous results were typically associated with patchy coastal cloud cover which either impacted the view of key kelp beds, or false positives associated with cloud cover or cloud shadow. The process was then repeated with those 8 dates excluded and data amalgamated by quarter (December – February, March – May, June – August, September – November) to produce temporally consistent datasets between sites. At each site a kelp presence absence map was produced across the analysed December 2015 to December 2024 date range.

2.2 Sea surface temperature and light attenuation

Sea surface temperatures (SST) were estimated using the NOAA "Optimum Interpolation Sea Surface Temperature (OISST) V2.1" product (Reynolds & Banzon 2008). This provides a 1/4 degree global, daily SST estimate from late 1981 to present. Daily SST and temperature anomaly (i.e., the daily OISST

minus a 30-year climatological mean) values from December 2015 to December 2024 were extracted from the NOAA OISST product.

The diffuse downwelling attenuation coefficient in the Photosynthetically Available Radiation (PAR range, 400-700 nm), Kd (m-1) was used as our measure of water clarity. Values of Kd were estimated from MODIS-Aqua measurements of ocean colour, processed to inherent optical properties using the QAA algorithm (Lee et al. 2002, 2009) following the methodology of Pinkerton et al. (2018). From these IOPs, we estimated the diffuse attenuation coefficient in the PAR range as Lee et al. (2005) and Shi & Wang (2007). The satellite-derived attenuation coefficient was mapped at a nominal resolution of 500×500 m and projected to a transverse Mercator grid. The temporal resolution of the product for the study region is 1-2 measurements daily. Values of Kd were extracted from the dataset around kelp forests and averaged monthly to provide a dataset with low quantities of missing data (Pinkerton et al. 2018).

2.3 Data analysis

The effects of monthly maximum SST, temperature anomaly, and water clarity (as defined by the light attenuation coefficient K_d) on *Macrocystis* cover were analysed with Generalized Additive Models (GAMs) using the "R" package "mgcv." Furthermore, GAMs were used separately to assess the potential for linear and non-linear covariance between physical parameters (temperature anomalies, light attenuation,). Assumptions of normality (Q-Q plot), homogeneity of variance (Levene's Test), as well as "concurvity" for general additive model analysis (an estimate of redundancy among explanatory variables) were checked for models. GAM models were fitted with "tp" (thin plate) splines, using a k-value of 6 (i.e., the number of "knots" denoting the complexity of the non-linear fit), and the distribution family "tweedie." Selection procedures were implemented to penalize and remove factors with poor explanatory power. The final model included mean monthly temperature, K_d , temperature anomaly, chl- α , and the two-way interaction between water clarity and temperature anomalies. Furthermore, the categorical variable "zone" was included in the GAM model.

Water temperatures were compared with temperature thresholds based on the known distribution limit of *Macrocystis* of 19°C (Hay 1990), and a threshold 2 degrees below that to show the possible effects of a predicted +2°C warmer world under global warming (Cheng et al. 2022).

3 RESULTS

3.1 National distribution and abundance of kelp

Macrocystis forests have been identified from central New Zealand to the sub-Antarctic Islands. Here we have created polygons that capture the biggest known beds, but also extensive areas of coastline that have the potential to encompass habitat for Macrocystis but have not been previously identified. These areas were associated with known environmental envelopes for Macrocystis. While we note instances that within individual passes or regions where aquatic vegetation other than pure Macrocystis beds are detected (e.g., estuarine macroalgae, beach cast algae, and rocky reef macroalgae), Macrocystis beds are the dominant aquatic vegetation in all areas selected.

Across New Zealand we show that there are an average of 2000 hectares of kelp forests, largely made up of *Macrocystis pyrifera*. Although it is not appropriate to make direct comparisons between areas given the variable size of coastline incorporated within each polygon, the Otago region (Waikouaiti-Oamaru) has the greatest coverage of *Macrocystis*, with almost 1000 hectares of *Macrocystis* alone (Figure 2). The Motunau and Timaru regions had the lowest coverage of *Macrocystis* but also represent the smallest polygons and some of the most discrete kelp beds across New Zealand.

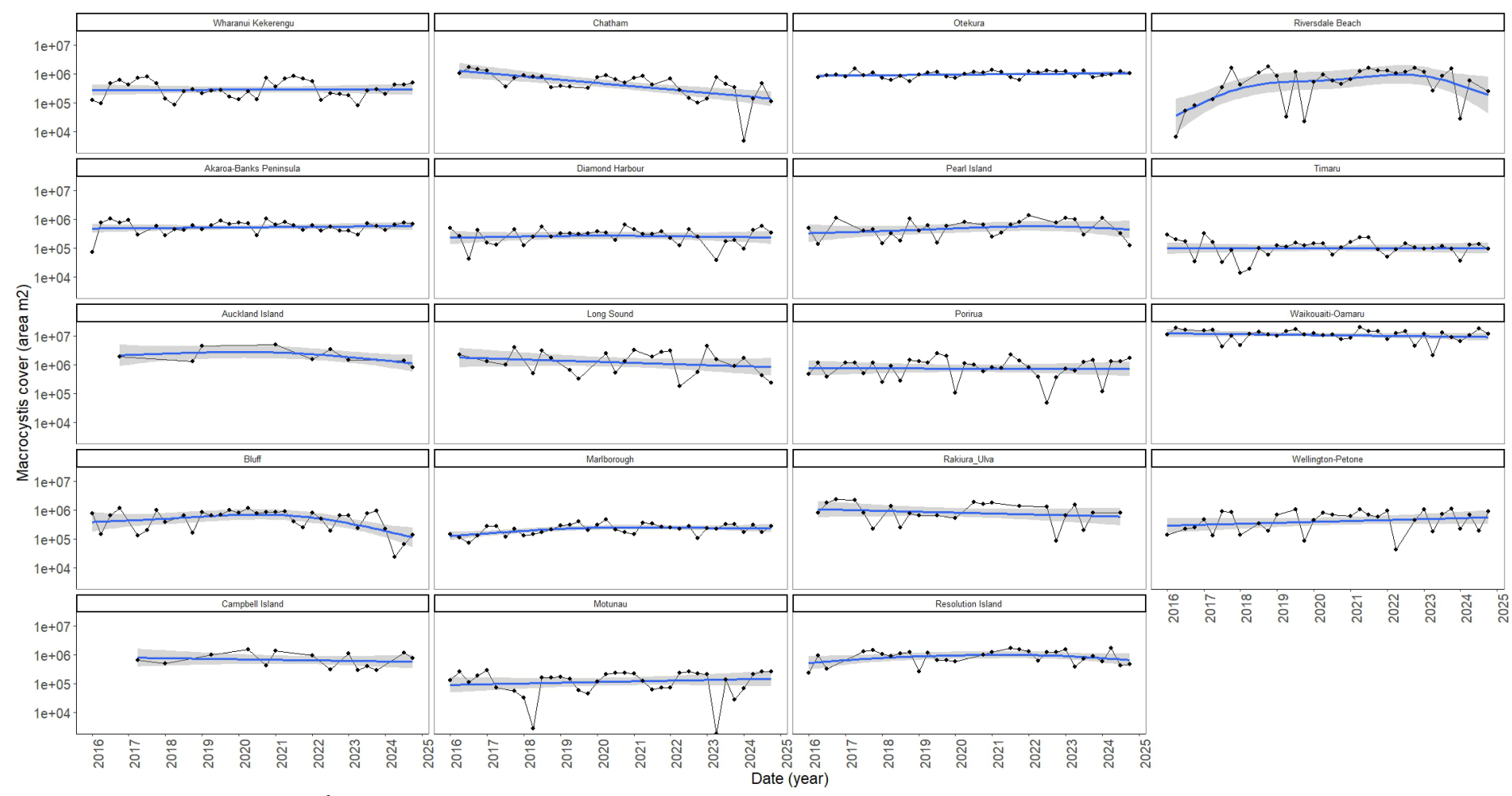


Figure 2: Cover of *Macrocystis* (m²) over the 10-year timeseries across individual regions throughout New Zealand and the sub-Antarctic Islands. Trends (blue line) are fitted by General Additive Models (GAM), including 95% confidence intervals (grey fill).

Region 1: Wellington, Marlborough Sounds

Central New Zealand represents the northern extent of *Macrocystis* distribution in New Zealand. Satellite imagery timeseries were processed for three regions, Porirua (Figure 3), Marlborough Sounds (Figure 4), and Wellington (Figure 5). Since little is known about *Macrocystis* beds in the region the area is represented by a relatively large exploratory polygon. Results showed that significant beds exist between Mana Island and the mainland (Figure 3). These beds are of significant extent but vary greatly in size across the timeseries. There was, however, a level of consistency of bed location over time (as indicated by moderately high proportional cover). There was also consistency in the proportional cover over time, including a rising trend in the past 1.5 years.

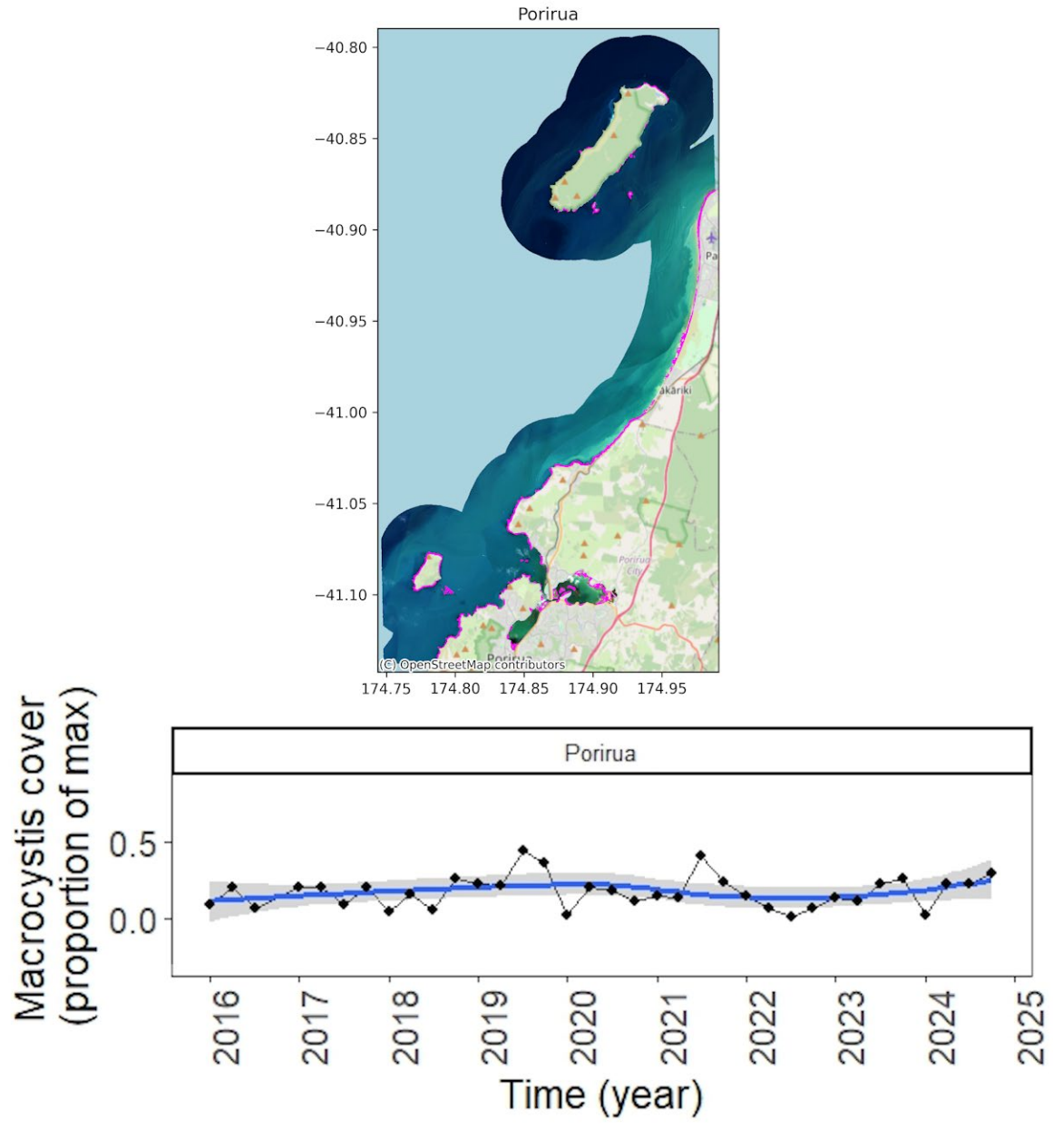


Figure 3: Combined distribution of kelp over the 10-year timeseries of Sentinel-2 imagery for the Porirua region. Map shows the area clipped for processing, including the removal of land and constant buffer around coastlines. Purple polygons show kelp detected. Bottom figure shows the coverage of kelp over time, presented as a proportion of the maximum coverage detected across the timeseries.

The Marlborough Sounds region is dominated by relatively narrow beds fringing the coastline (Figure 4). The locations analysed here show two key regions where kelp is detected, Tory Channel, and Motuara Island/ Outer Queen Charlotte Sound. While the *Macrocystis* beds at the northern tip of Motuara Island were some of the biggest individual beds, the overall coverage of *Macrocystis* in Tory Channel was greater. Overall, there was very low cover of *Macrocystis*, especially compared to the overall maximum cover, which suggests that these beds occurred sporadically in space and time. There were no obvious trends over the 10-year timeseries.

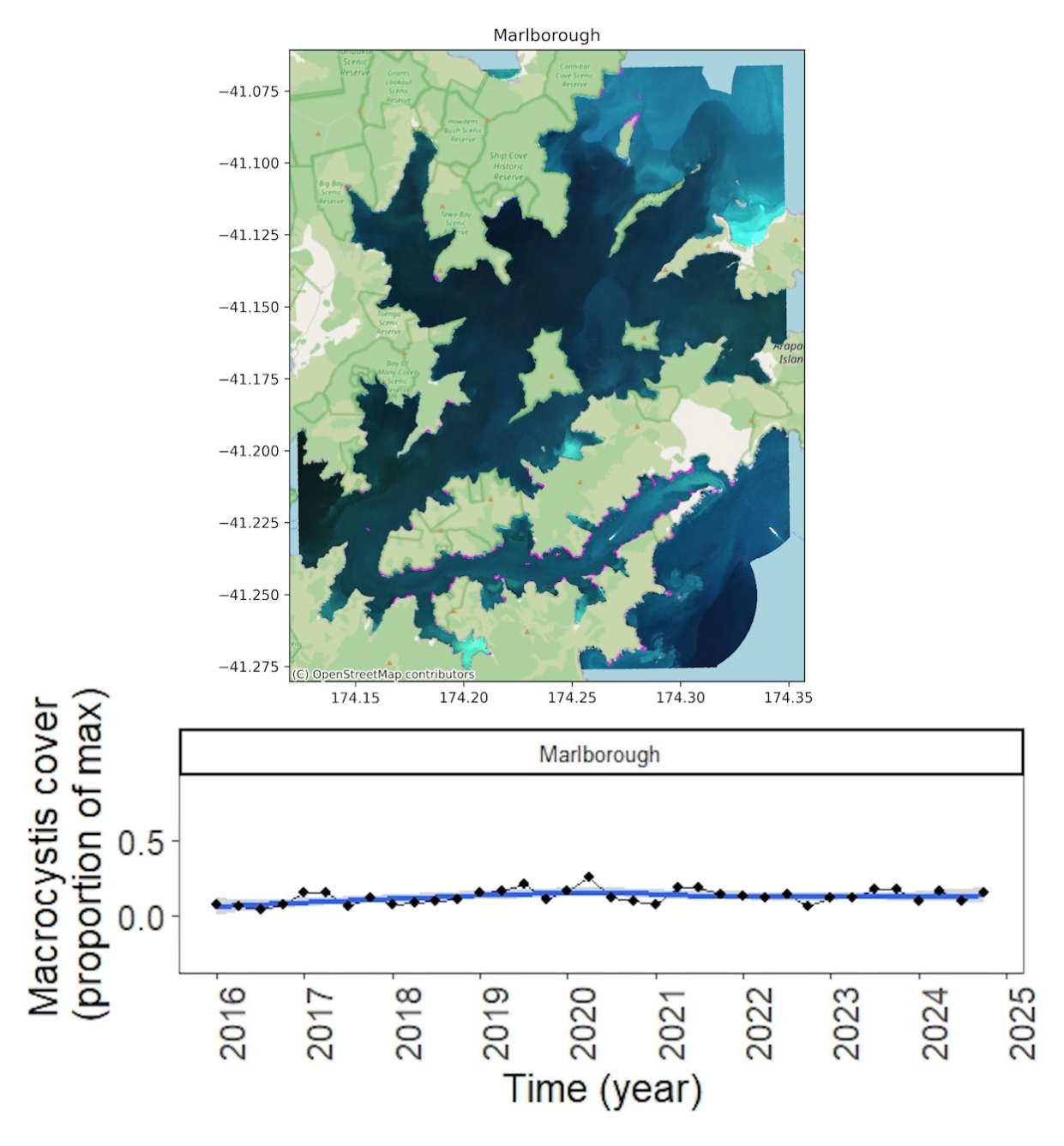


Figure 4: Combined distribution of kelp over the 10-year timeseries of Sentinel-2 imagery for the Marlborough region. Map shows the area clipped for processing, including the removal of land and constant buffer around coastlines. Purple polygons show kelp detected. Bottom figure shows the coverage of kelp over time, presented as a proportion of the maximum coverage detected across the timeseries.

Macrocystis beds within and surrounding Wellington Harbour showed significant beds surrounding Lyall Bay, on the south-western side of Wellington Harbour and the Eastern Coast of Wellington Harbour (Figure 5). The coverage of these beds varied dramatically through time, although there was some consistency in the locations of kelp through time (as shown by relatively high proportional cover). There were no obvious trends over the 10-year timeseries.

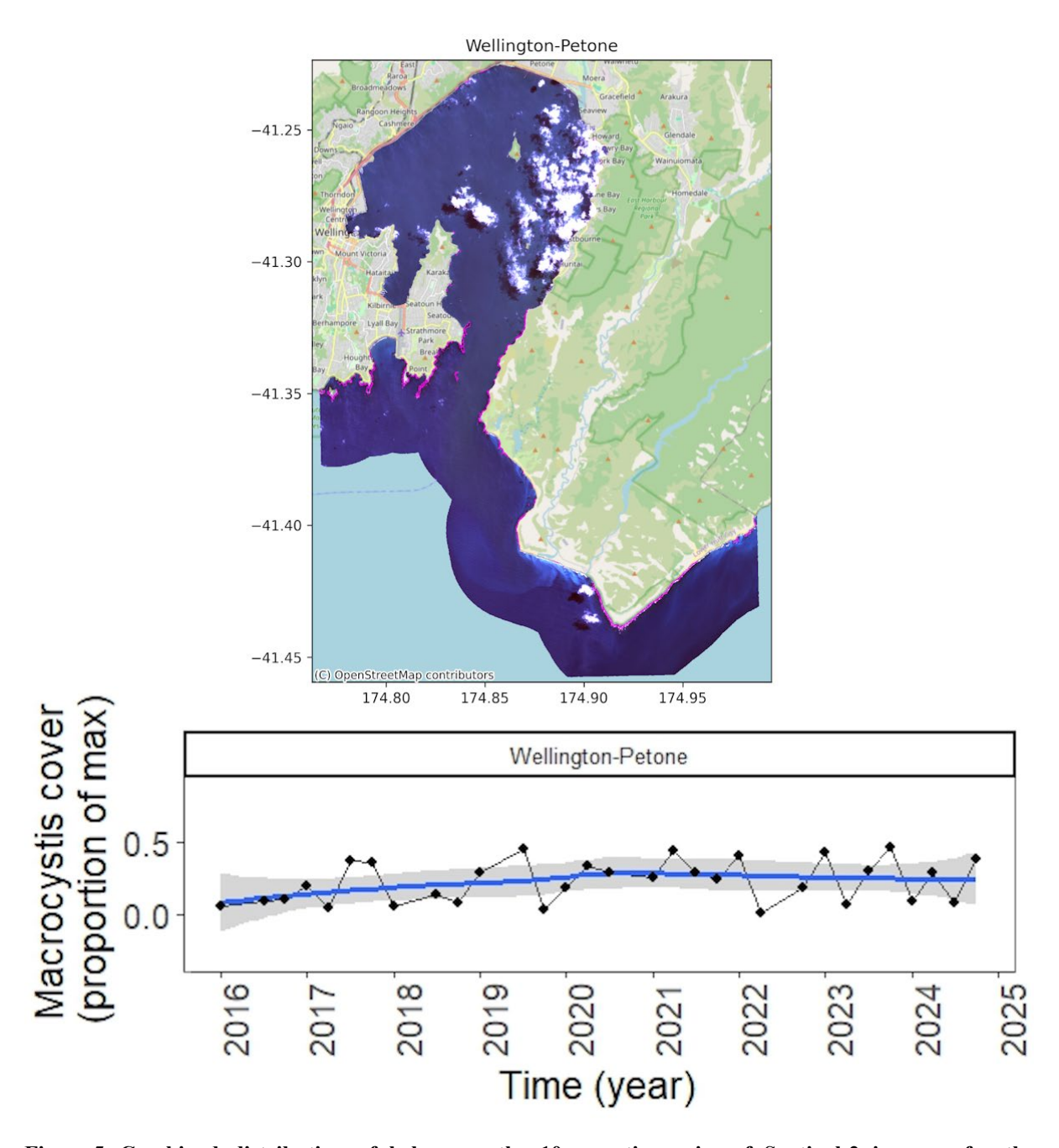


Figure 5: Combined distribution of kelp over the 10-year timeseries of Sentinel-2 imagery for the Wellington region. Map shows the area clipped for processing, including the removal of land and constant buffer around coastlines. Purple polygons show kelp detected. Bottom figure shows the coverage of kelp over time, presented as a proportion of the maximum coverage detected across the timeseries.

Region 2: Kaikōura and Canterbury

The Canterbury and Kaikoura coastline is represented by five discreet areas, the Wharanui/ Kekerengu (northern Kaikoura) region (Figure 6), Motunau Island (Figure 7), the Diamond Harbour (northern Banks Peninsula, Figure 8) region, Akaroa Harbour (Figure 9), and the Timaru (Figure 10) region. The *Macrocystis* abundance and distribution of the Wharanui/ Kekerengu region is poorly described and relatively unknown. Our results show significant beds north of the Clarence River mouth (Figure 6). Although these beds are at times quite large, they are relatively sporadic in time and at times are completely absent at the surface. There were no obvious trends over the 10-year timeseries.

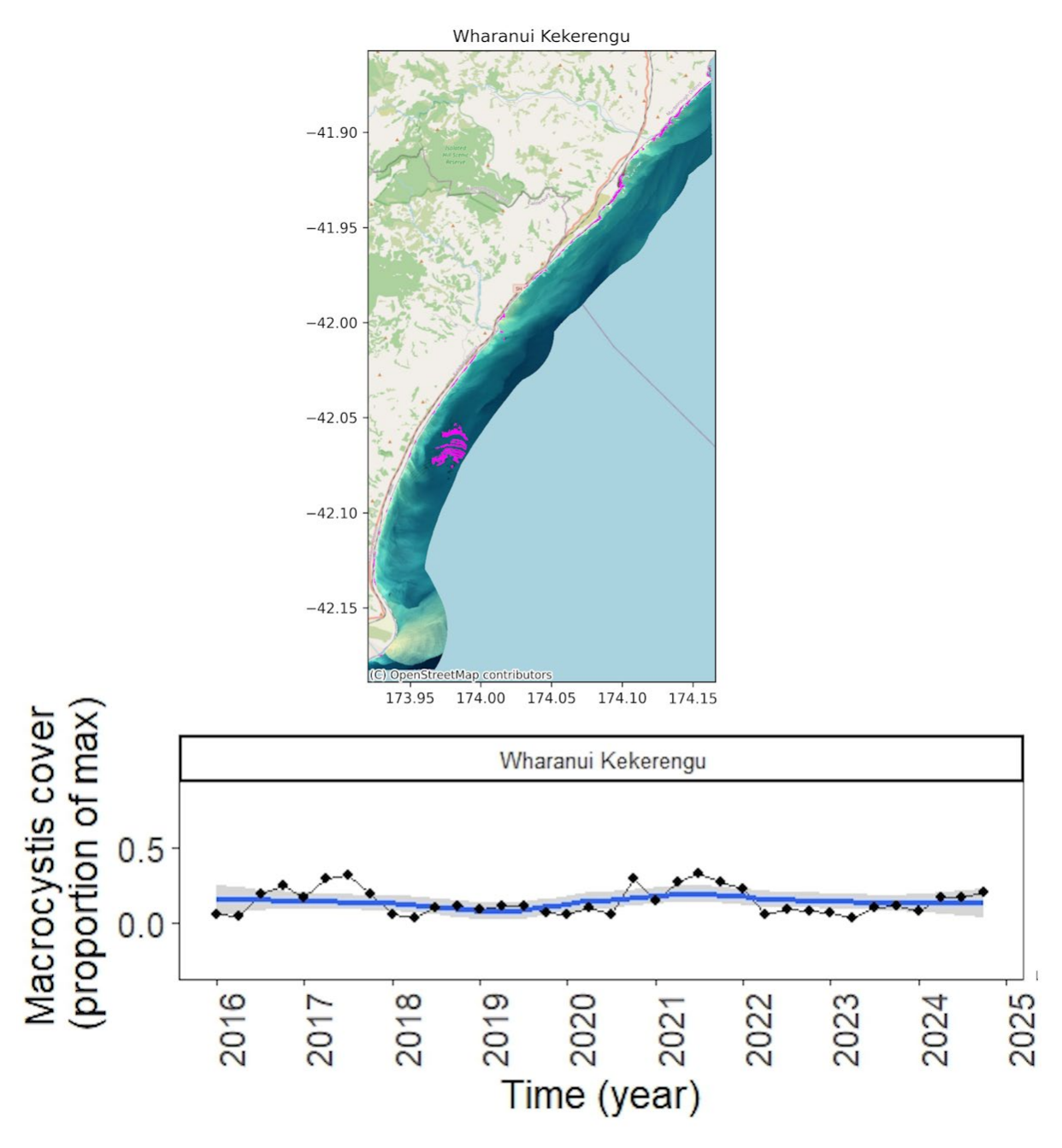


Figure 6: Combined distribution of kelp over the 10-year timeseries of Sentinel-2 imagery for the Wharanui/Kekerengu (Northern Kaikōura region) region. Map shows the area clipped for processing, including the removal of land and constant buffer around coastlines. Purple polygons show kelp detected. Bottom figure shows the coverage of kelp over time, presented as a proportion of the maximum coverage detected across the timeseries.

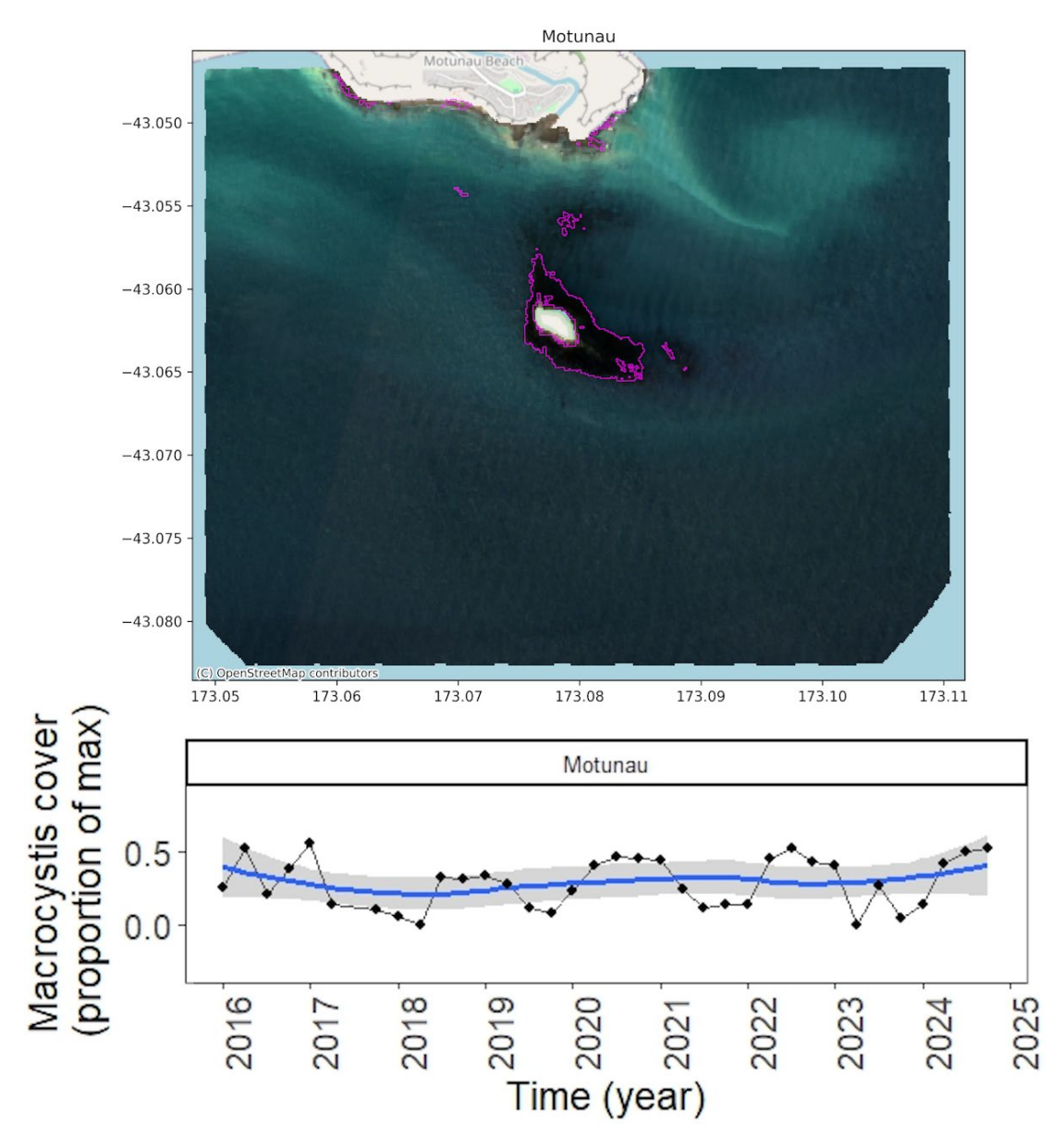


Figure 7: Combined distribution of kelp over the 10-year timeseries of Sentinel-2 imagery for the Motunau region. Map shows the area clipped for processing, including the removal of land and constant buffer around coastlines. Purple polygons show kelp detected. Bottom figure shows the coverage of kelp over time, presented as a proportion of the maximum coverage detected across the timeseries.

Although there are sporadic *Macrocystis* beds between Kaikōura and Banks Peninsula, some of the largest and most consistent beds occur at Motunau Island (Figure 7). Although there are signals of interannual variability, these beds are discrete and consistent in where they are detected. Motunau Island had relatively high cover (i.e., as a proportion of the maximum extent) indicating that beds were frequently covering a large proportion of the maximum extent. This shows that this bed was relatively discrete, and somewhat consistent in where kelp was detected.

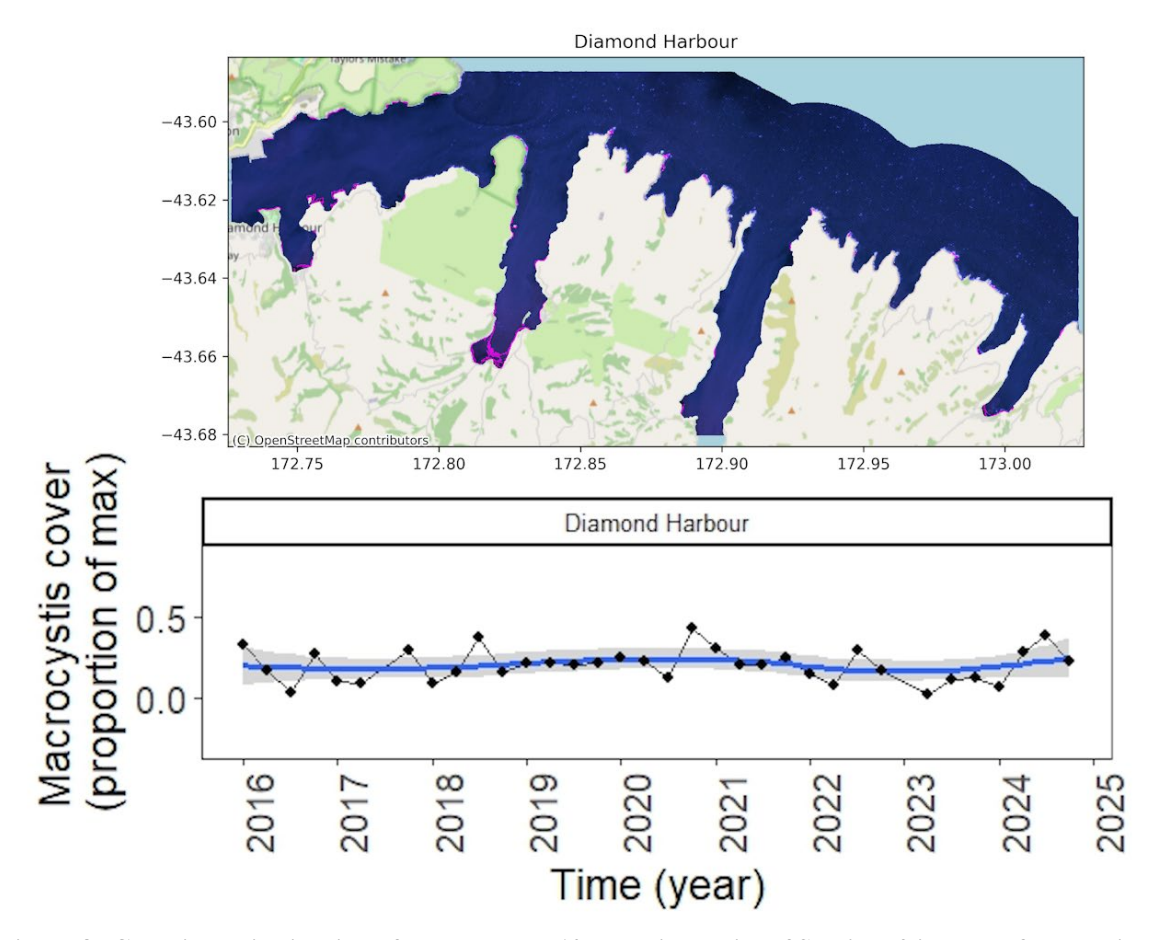


Figure 8: Combined distribution of kelp over the 10-year timeseries of Sentinel-2 imagery for the Diamond Harbour (northern Banks Peninsula) region. Map shows the area clipped for processing, including the removal of land and constant buffer around coastlines. Purple polygons show kelp detected. Bottom figure shows the coverage of kelp over time, presented as a proportion of the maximum coverage detected across the timeseries.

The Diamond Harbour region (northern Banks Peninsula) is defined by relatively small kelp beds within Lyttelton Harbour and sporadic beds surrounding headlands to the east (Figure 8). Although there are some peaks in proportional cover, overall, the trends show that the presence of kelp beds are relatively sporadic over time. There were no obvious trends over the 10-year timeseries.

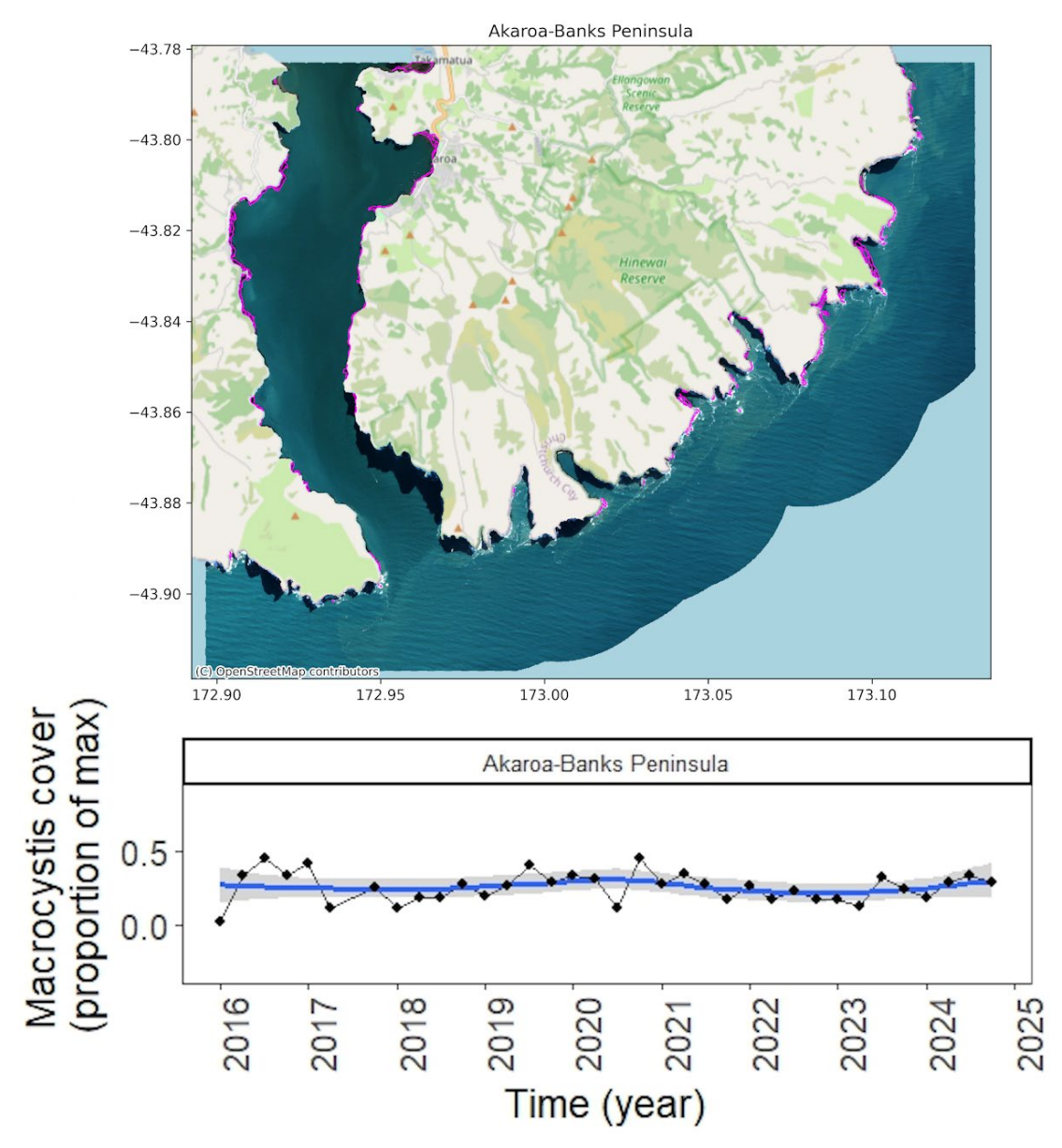
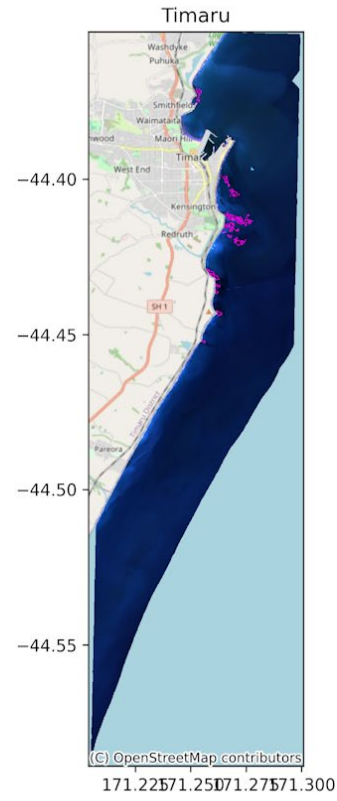


Figure 9: Combined distribution of kelp over the 10-year timeseries of Sentinel-2 imagery for the Akaroa (southern Banks Peninsula) region. Map shows the area clipped for processing, including the removal of land and constant buffer around coastlines. Purple polygons show kelp detected. Bottom figure shows the coverage of kelp over time, presented as a proportion of the maximum coverage detected across the timeseries.

The Akaroa region (southern Banks Peninsula) is defined by moderate kelp beds within Akaroa Harbour and surrounding bays to the east (Figure 9). Overall trends show that the presence of kelp beds is relatively consistent over time. There were no obvious trends over the 10-year timeseries.

The Timaru region is defined by moderate sized *Macrocystis* beds on offshore rocky reef platforms (Figure 10). These beds are adjacent to Timaru itself and surrounding headlands to the south. The abundance of *Macrocystis* shows some seasonal trends but appear to be relatively sporadic over time. There was a weak trend of declining cover over the 10-year timeseries.



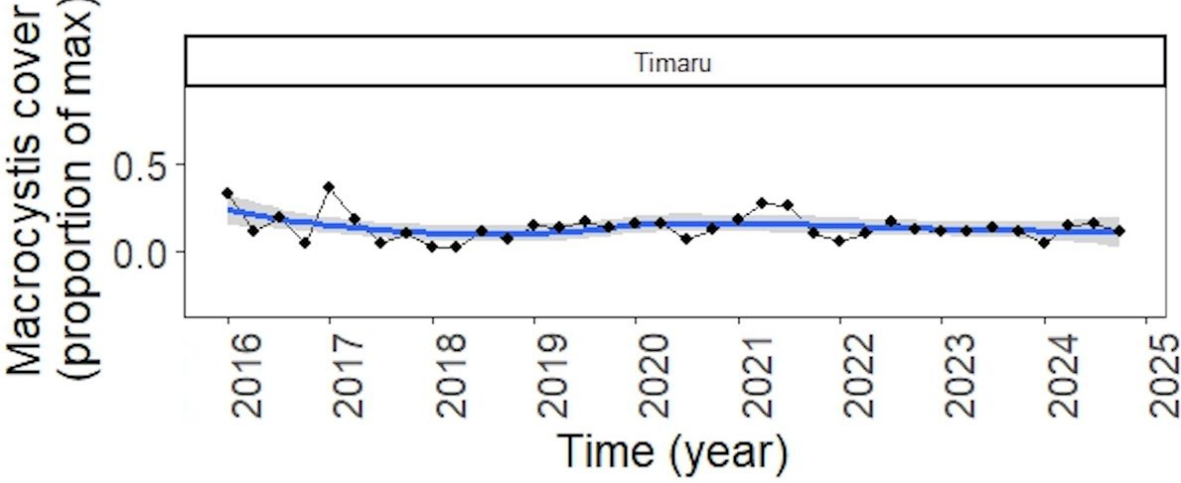


Figure 10: Combined distribution of kelp over the 10-year timeseries of Sentinel-2 imagery for the Timaru region. Map shows the area clipped for processing, including the removal of land and constant buffer around coastlines. Purple polygons show kelp detected. Bottom figure shows the coverage of kelp over time, presented as a proportion of the maximum coverage detected across the timeseries.

Region 3: Chatham Islands

The Chatham Islands have significant populations of *Macrocystis*, including throughout bays on the northwestern portion of Chatham Island, large beds at the northeastern tip and beds throughout the southern part of Chatham Island, and surrounding Pitt Island (Figure 11). During the 10-year timeseries there was a decline in the cover of *Macrocystis*.

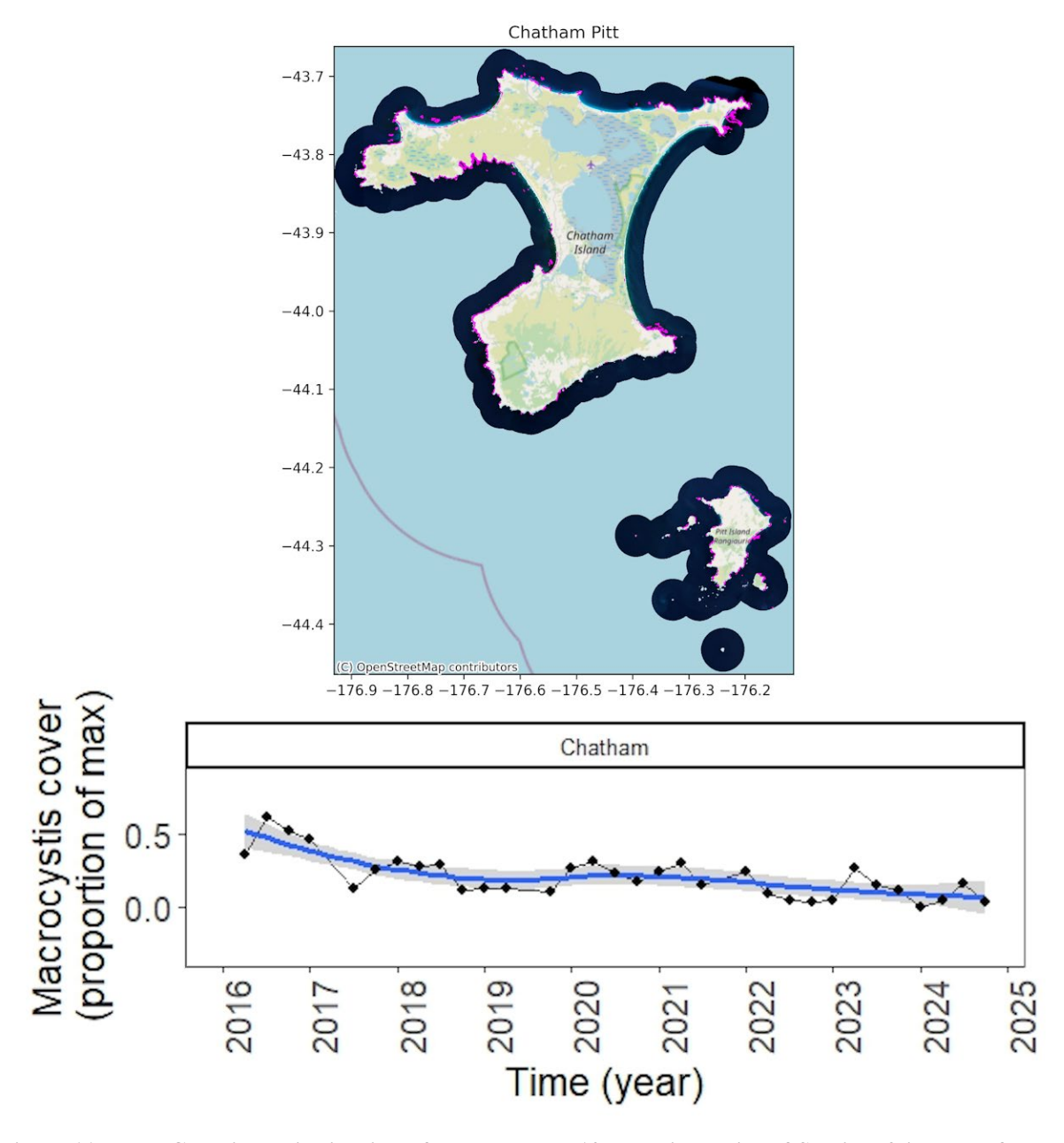


Figure 11: Combined distribution of kelp over the 10-year timeseries of Sentinel-2 imagery for the Chatham (and Pitt) Island region. Map shows the area clipped for processing, including the removal of land and constant buffer around coastlines. Purple polygons show kelp detected. Bottom figure shows the coverage of kelp over time, presented as a proportion of the maximum coverage detected across the timeseries.

Region 4: Otago

The Otago region has some of the most extensive *Macrocystis* populations in the country (Figure 12). This region is represented by the north Otago region spanning the Otago Peninsula to Oamaru (Figuer 12), and a more discrete region surrounding Nugget Point (Figure 13). In particular, the beds north of the Otago Peninsula surrounding Waikouaiti are some of the largest and most consistent beds in New Zealand (Figure 12). Large and distinct *Macrocystis* beds occur on offshore reefs from Waikouaiti to the Moeraki Peninsula. These beds also show high fidelity with consistently high proportional cover. There were no obvious trends over the 10-year timeseries, however, proportional cover was increasingly variable since 2021.

Waikouaiti-Oamaru

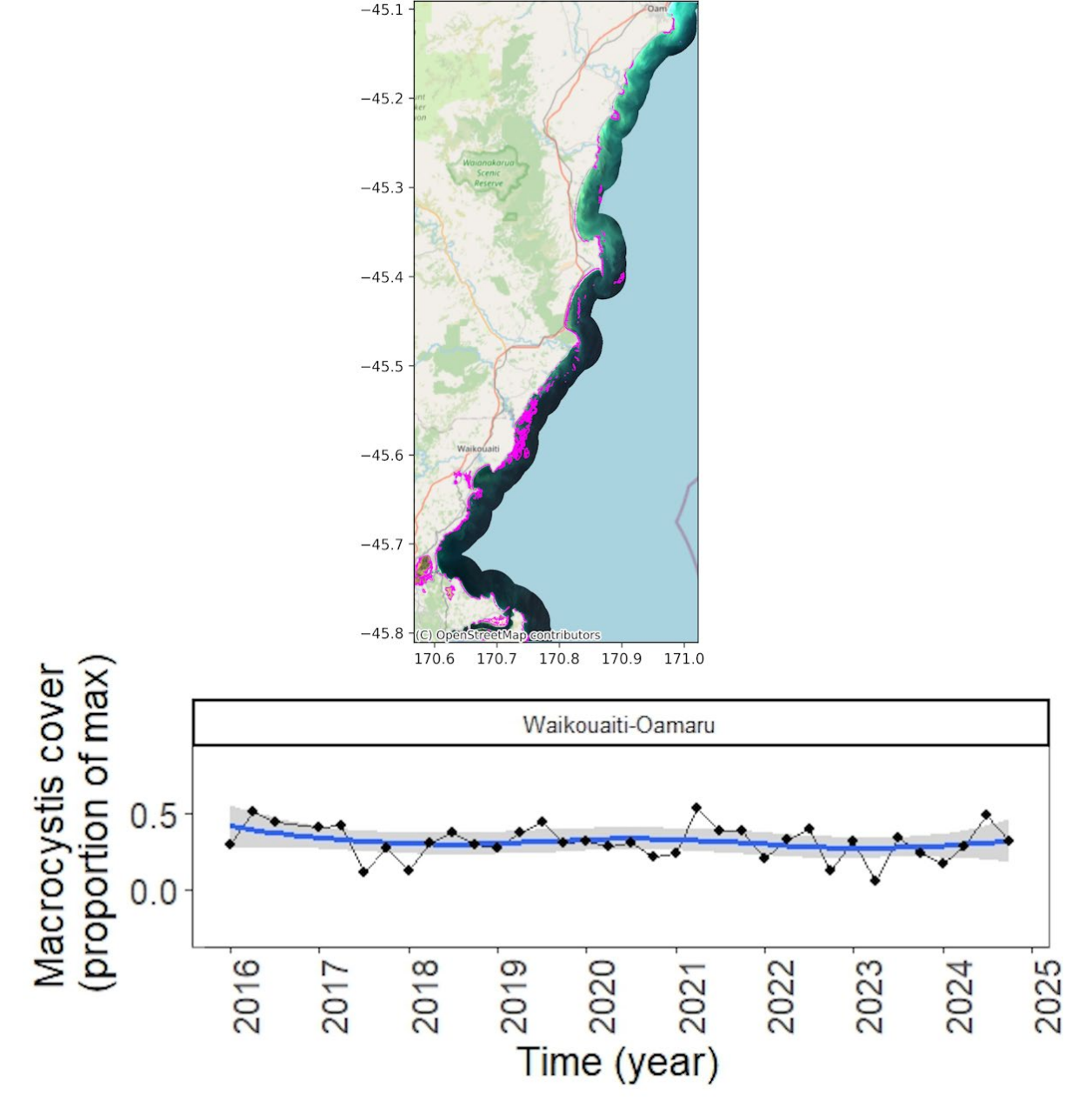


Figure 12: Combined distribution of kelp over the 10-year timeseries of Sentinel-2 imagery for the Waikouaiti/Oamaru (north Otago) region. Map shows the area clipped for processing, including the removal of land and constant buffer around coastlines. Purple polygons show kelp detected. Bottom figure shows the coverage of kelp over time, presented as a proportion of the maximum coverage detected across the timeseries.

The Otekura regions of southern Otago includes Nugget Point and the mouth of the Catlins Estuary. *Macrocystis* beds in this region are primarily made up of beds to the north of Nugget Point, and beds within the mouth of the Catlins Estuary (Figure 13). Kelp beds detected in this region are also likely to include other species such as Durvillaea (i.e., southern bull kelp). *Macrocystis* beds were relatively consistent in their location (moderate proportional covers). There was a slight trend of increasing kelp cover over the 10-year timeseries.

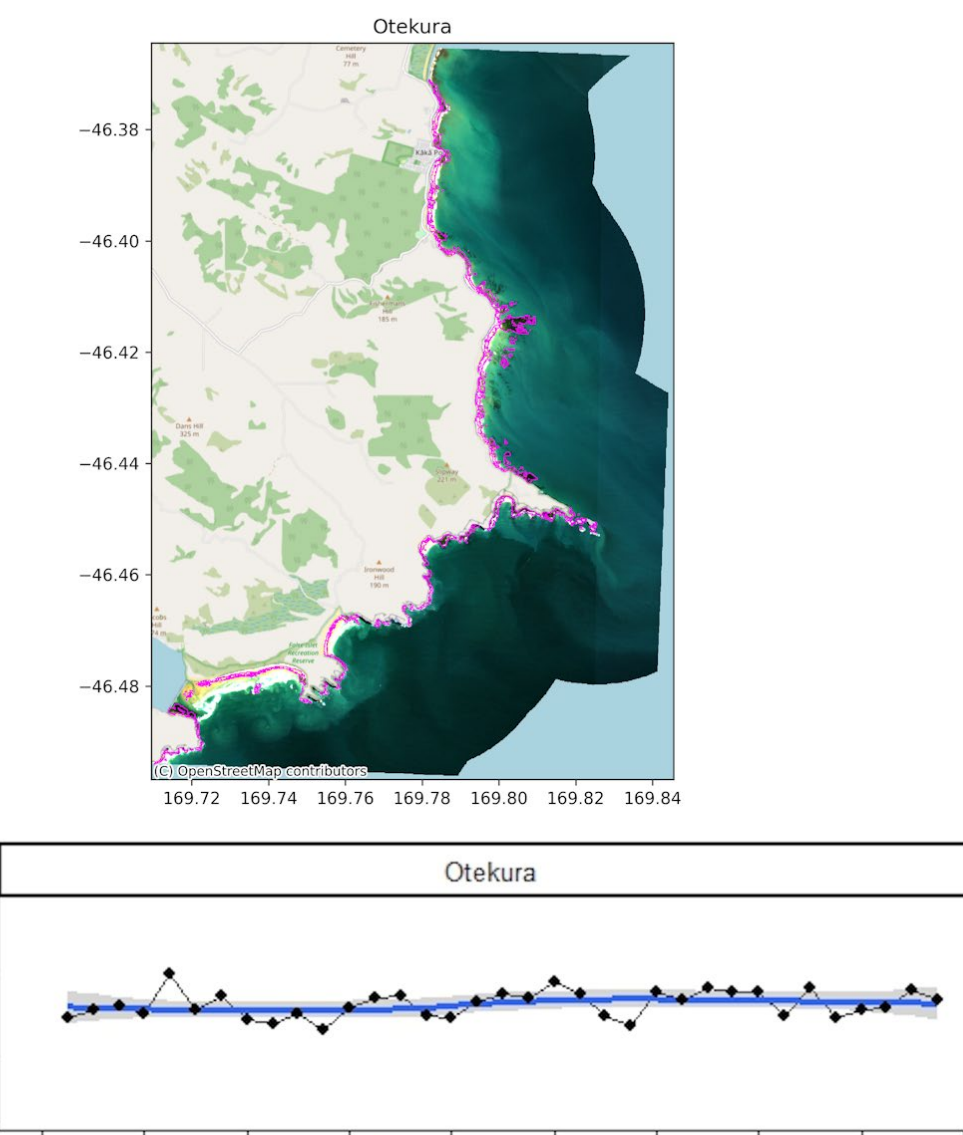


Figure 13: Combined distribution of kelp over the 10-year timeseries of Sentinel-2 imagery for the Otekura (south Otago/ Catlins) region. Map shows the area clipped for processing, including the removal of land and constant buffer around coastlines. Purple polygons show kelp detected. Bottom figure shows the coverage of kelp over time, presented as a proportion of the maximum coverage detected across the timeseries.

Time (year)

2018

proportion of max

0.5

0.0

Region 5: Southland, Fiordland and Rakiura

Southern New Zealand kelp beds are abundant and widely distributed across the region. Major beds exist within areas of southern Fiordland (Figure 14), surrounding Bluff Harbour (Figure 15), and Rakiura (Stewart Island, Figure 16, Figure 17). The region of Fiordland surrounding Resolution Island is dominated by *Macrocystis* beds inside the fiords in semi-protected areas (Figure 14). The detections also likely include other species such as Durvillaea, especially on the outer exposed coastlines. Locations of kelp beds had relatively low fidelity, as identified by the relatively low proportional cover. There were no obvious trends over the 10-year timeseries.

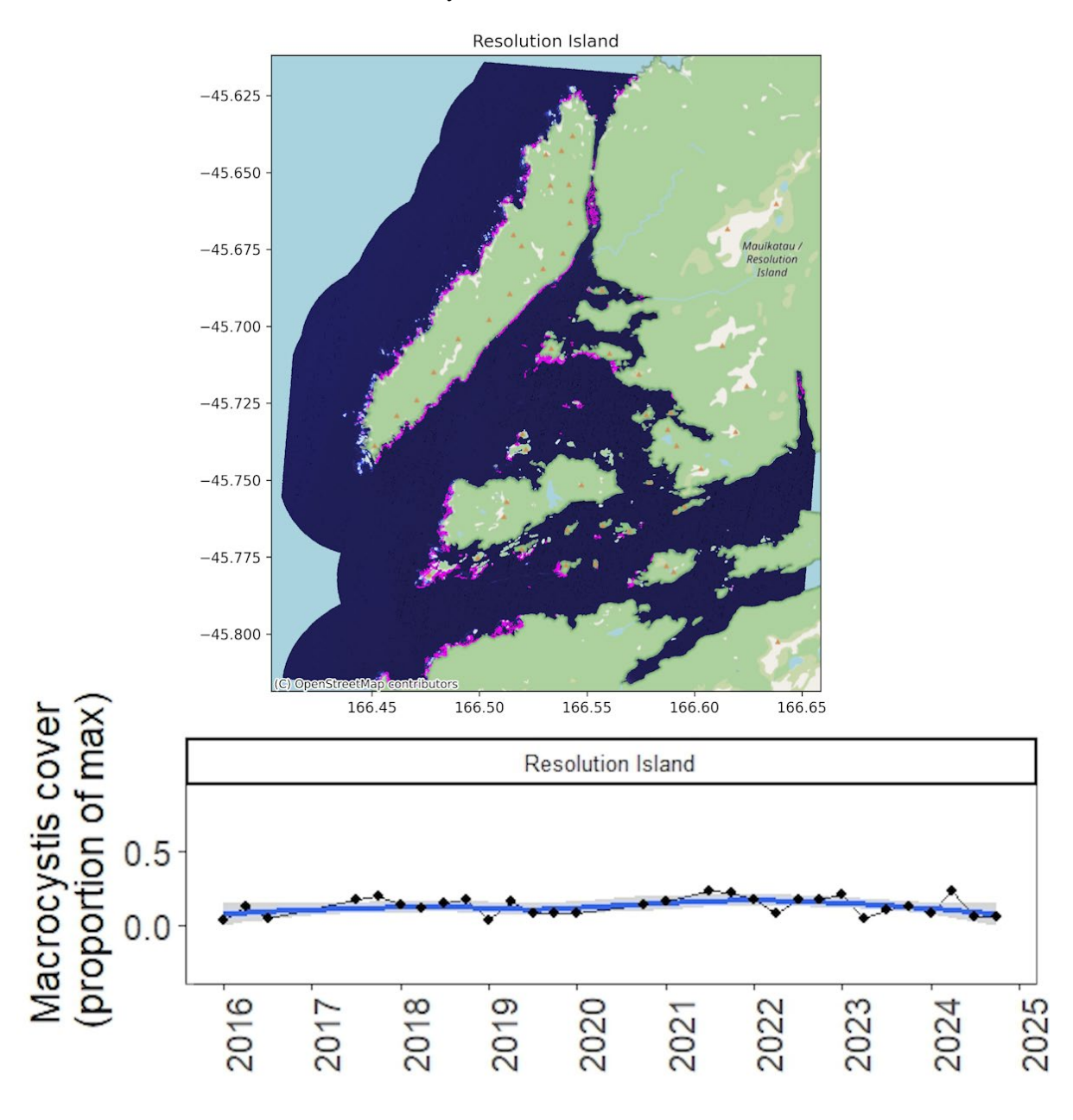


Figure 14: Combined distribution of kelp over the 10-year timeseries of Sentinel-2 imagery for the Resolution Island (Fiordland) region. Map shows the area clipped for processing, including the removal of land and constant buffer around coastlines. Purple polygons show kelp detected. Bottom figure shows the coverage of kelp over time, presented as a proportion of the maximum coverage detected across the timeseries.

The Long Sound region in southern Fiordland is dominated by coastal kelp beds, with some larger populations of *Macrocystis* surrounding rocky outcrops and islands (e.g., Pukahereka Island) within the sheltered fiords (Figure 15). However, we note that there are apparent kelp detections deep within the fiords that are unable to be confirmed as kelp beds. These significant detections led to the two highest dates for kelp coverage (Spring 2017, and Summer 2023) and may be artificially elevated due to these detections. Further work on the spectral signatures or additional *in situ* ground truthing is required to examine the validity of these detections.

Locations of kelp beds had moderate fidelity, as identified by the proportional cover over time. Fidelity may increase depending on the findings relating to the inner fiord detections. There was a trend of declining kelp cover over the 10-year timeseries.

Long Sound

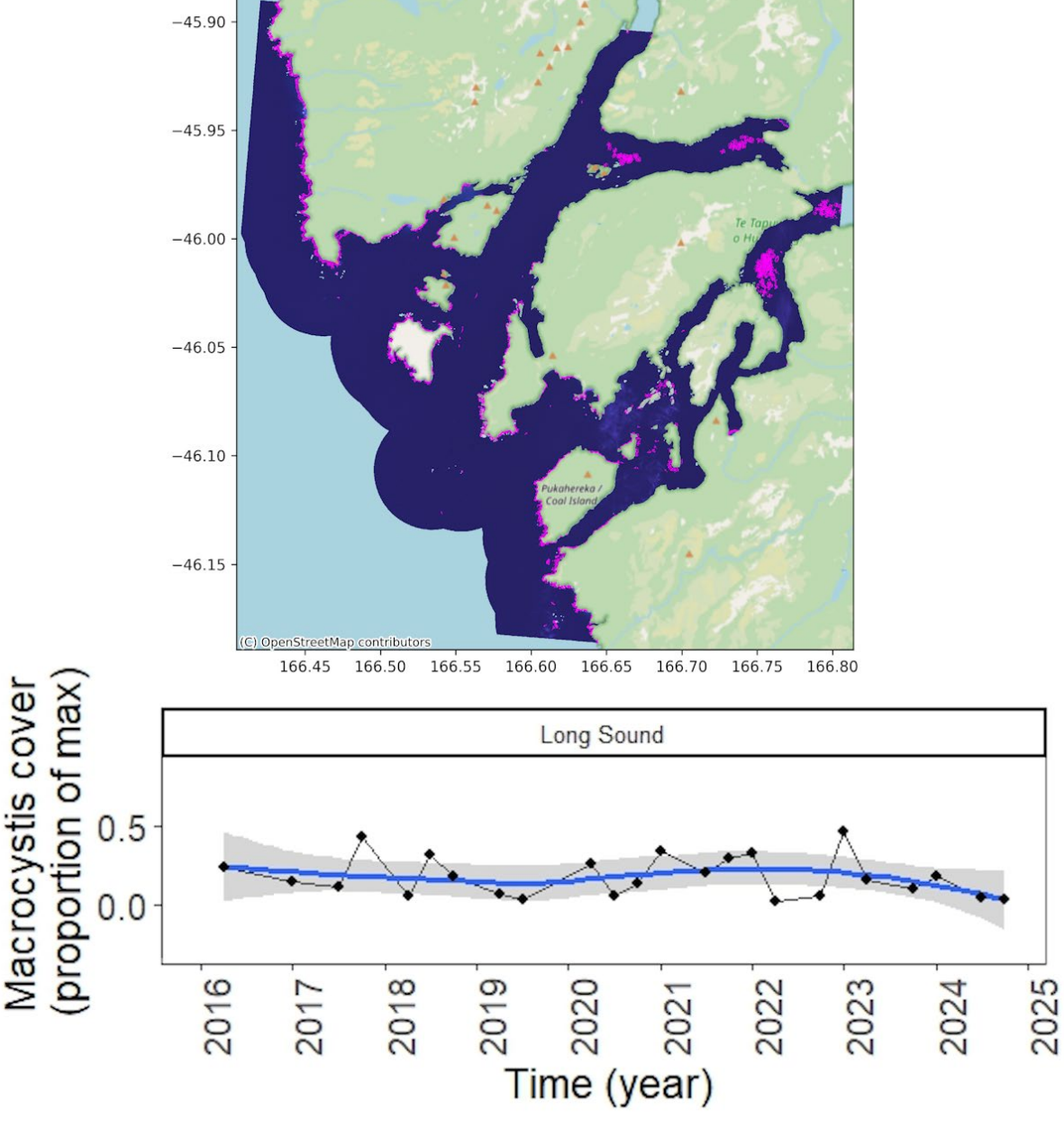


Figure 15: Combined distribution of kelp over the 10-year timeseries of Sentinel-2 imagery for the Long Sound (Fiordland) region. Map shows the area clipped for processing, including the removal of land and constant buffer around coastlines. Purple polygons show kelp detected. Bottom figure shows the coverage of kelp over time, presented as a proportion of the maximum coverage detected across the timeseries.

The region surrounding Bluff Harbour has extensive *Macrocystis* beds surrounding each side of the mouth of the Harbour, and further offshore surrounding Dog Island (Figure 16). These beds showed high fidelity, although there was high variability in proportional cover over time. There was a trend of declining kelp cover over the 10-year timeseries.

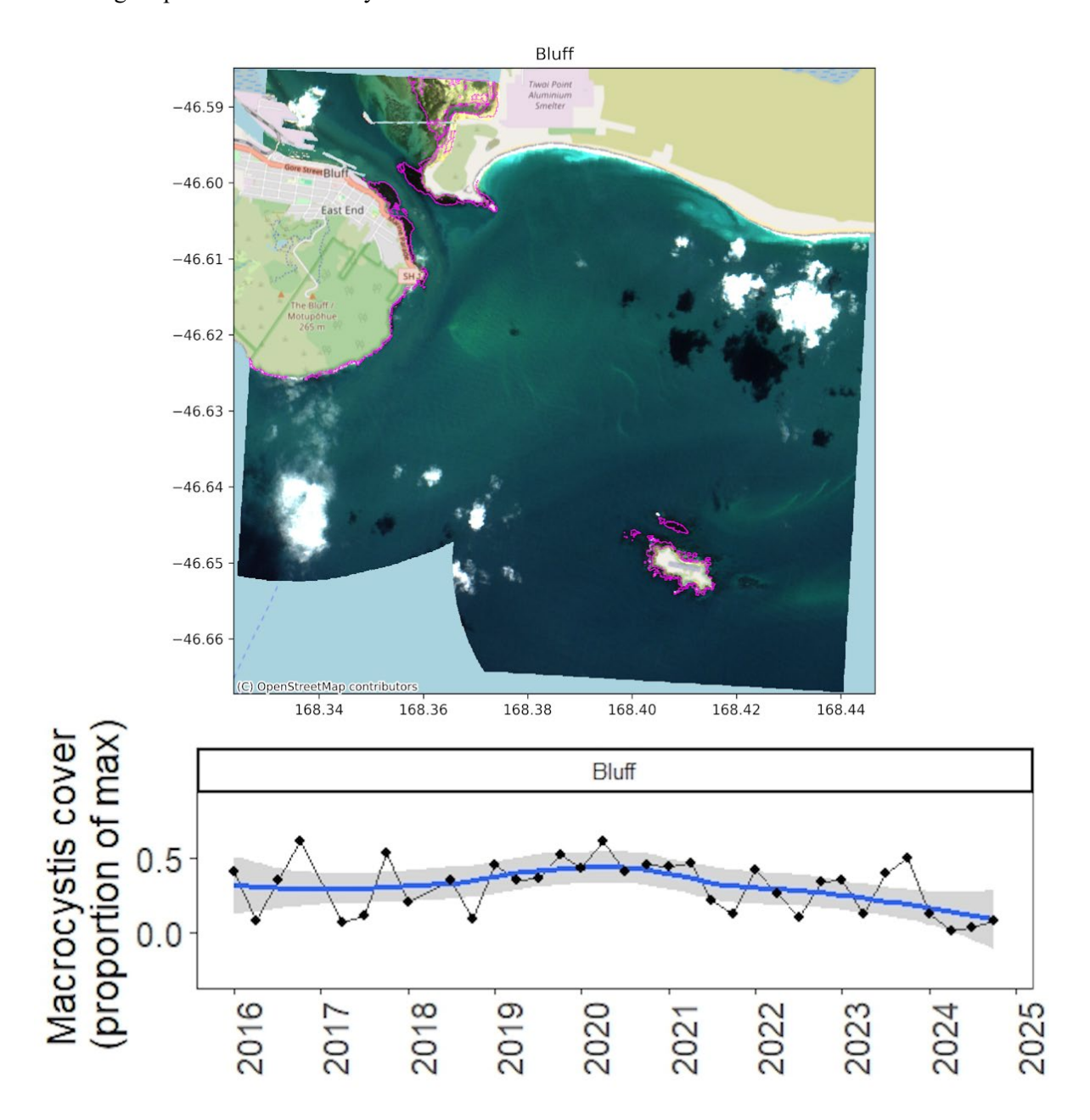
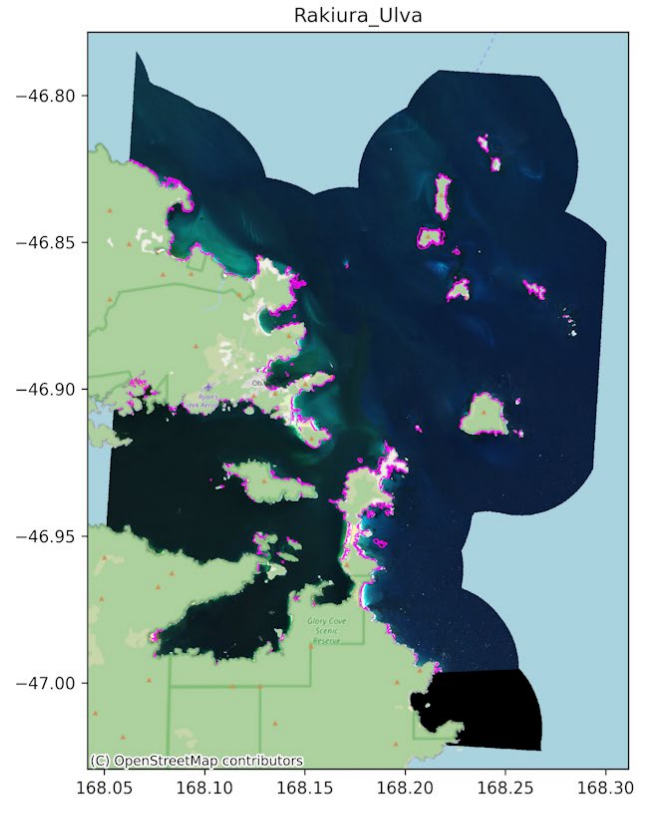


Figure 16: Combined distribution of kelp over the 10-year timeseries of Sentinel-2 imagery for the Bluff region. Map shows the area clipped for processing, including the removal of land and constant buffer around coastlines. Purple polygons show kelp detected. Bottom figure shows the coverage of kelp over time, presented as a proportion of the maximum coverage detected across the timeseries.

The region surrounding northern Rakiura has large kelp beds on the bays and peninsulas of Rakiura, but also significant populations on surrounding offshore islands (Figure 17). These beds had moderate fidelity at times, but also periods of very low fidelity and large declines of cover. There was a slight trend of declining cover over the 10-year timeseries.



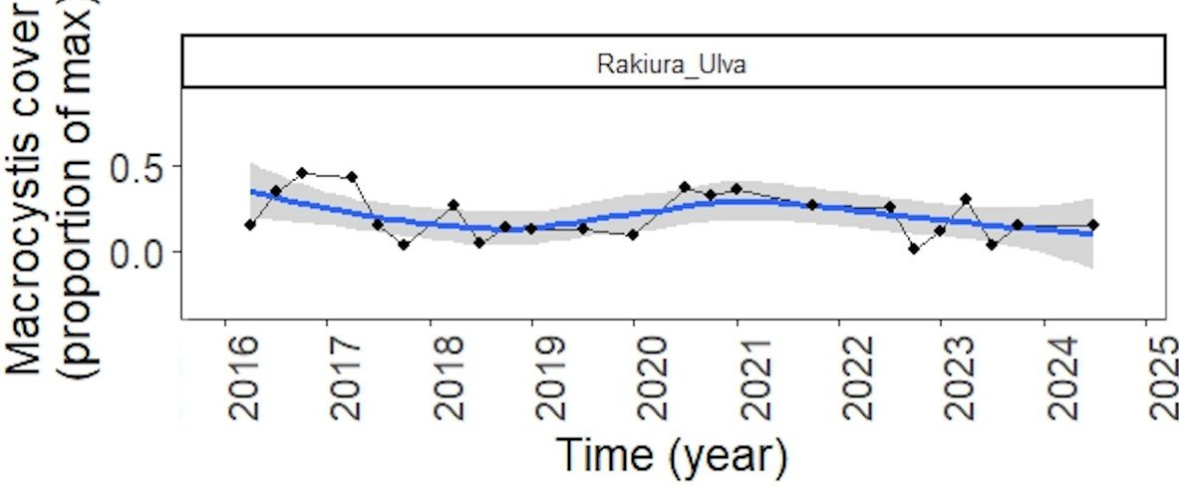


Figure 17: Combined distribution of kelp over the 10-year timeseries of Sentinel-2 imagery for Rakiura/ Ulva Island region. Map shows the area clipped for processing, including the removal of land and constant buffer around coastlines. Purple polygons show kelp detected. Bottom figure shows the coverage of kelp over time, presented as a proportion of the maximum coverage detected across the timeseries.

The southern region of Rakiura centred on Pearl Island and Port Pegasus was dominated by kelp beds fringing the coastline (Figure 18). Like northern Rakiura the kelp beds had moderate to low fidelity, with many periods of low kelp cover. There was no obvious trend of kelp cover of the 10-year timeseries.

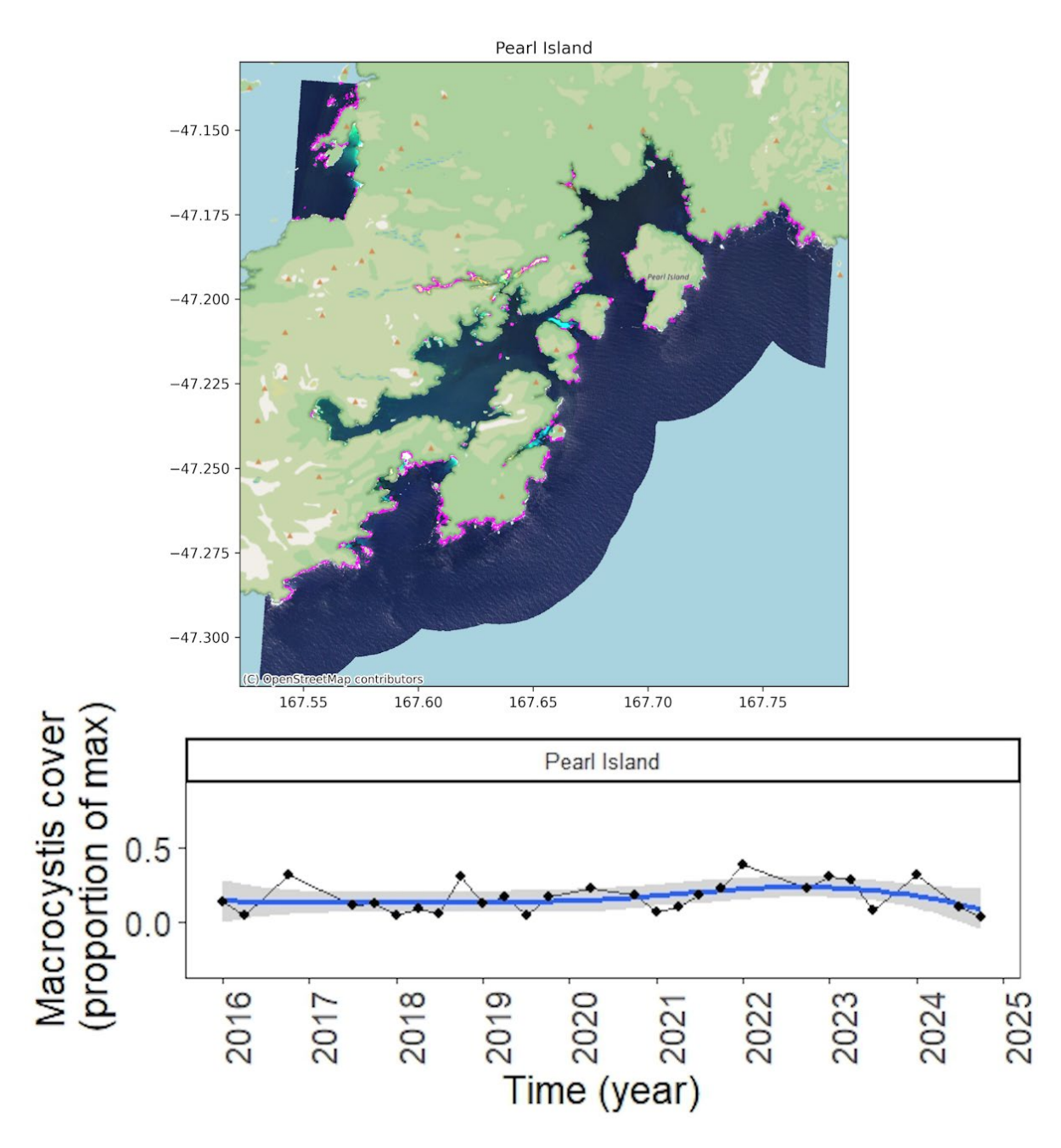


Figure 18: Combined distribution of kelp over the 10-year timeseries of Sentinel-2 imagery for Pearl Island (Port Pegasus, Rakiura) region. Map shows the area clipped for processing, including the removal of land and constant buffer around coastlines. Purple polygons show kelp detected. Bottom figure shows the coverage of kelp over time, presented as a proportion of the maximum coverage detected across the timeseries.

Region 6: Sub-Antarctic Islands

The sub-Antarctic region is represented by the two major sub-Antarctic islands within New Zealand's EEZ, Auckland Island (Figure 19), and Campbell Island (Figure 20). Usable satellite imagery for the sub-Antarctic islands is limited due to reduced reflectance signals during the winter months, but also high proportions of cloud cover. Consequently, measures of kelp cover over the 10-year timeseries are limited and sporadic. Auckland Island has extensive *Macrocystis* beds within sheltered bays on the East Coast, including within Port Ross, and on the northeastern region of the Island (Figure 19). The beds

had relatively high fidelity at times, but also periods of significantly lower cover of kelp, especially since 2023. Although the low number of usable satellite passes makes identifying trends difficult, there was a weak trend of declining cover since 2021.

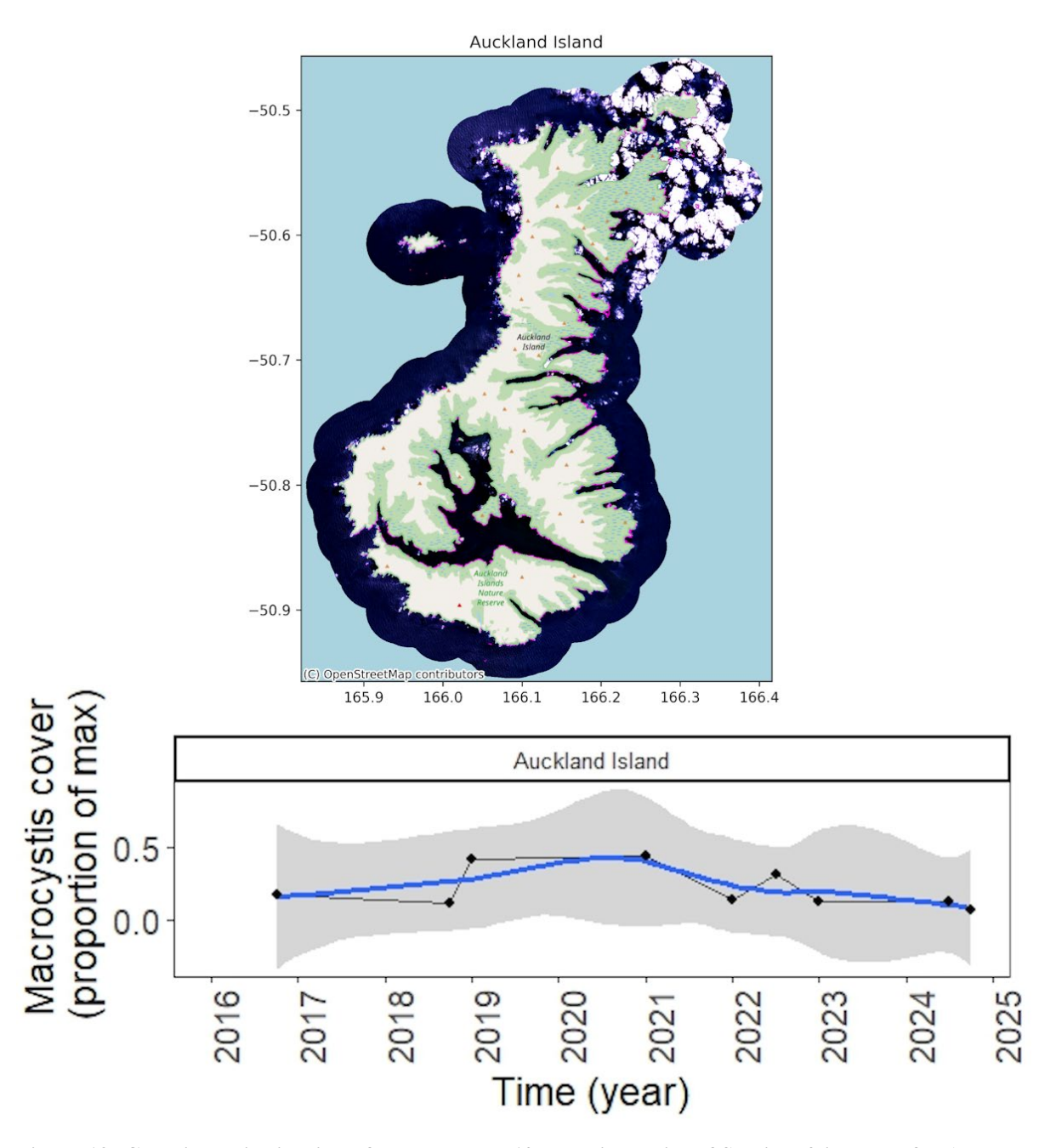


Figure 19: Combined distribution of kelp over the 10-year timeseries of Sentinel-2 imagery for Auckland Island. Map shows the area clipped for processing, including the removal of land and constant buffer around coastlines. Purple polygons show kelp detected. Bottom figure shows the coverage of kelp over time, presented as a proportion of the maximum coverage detected across the timeseries.

Campbell Island had significant kelp beds surrounding the northeast region of the Island, including within Perseverance Harbour, and a notable bed in a semi-sheltered bay on the southwest coast (Figure 20). Kelp bed location had relatively low fidelity. There were no obvious trends over the 10-year timeseries.

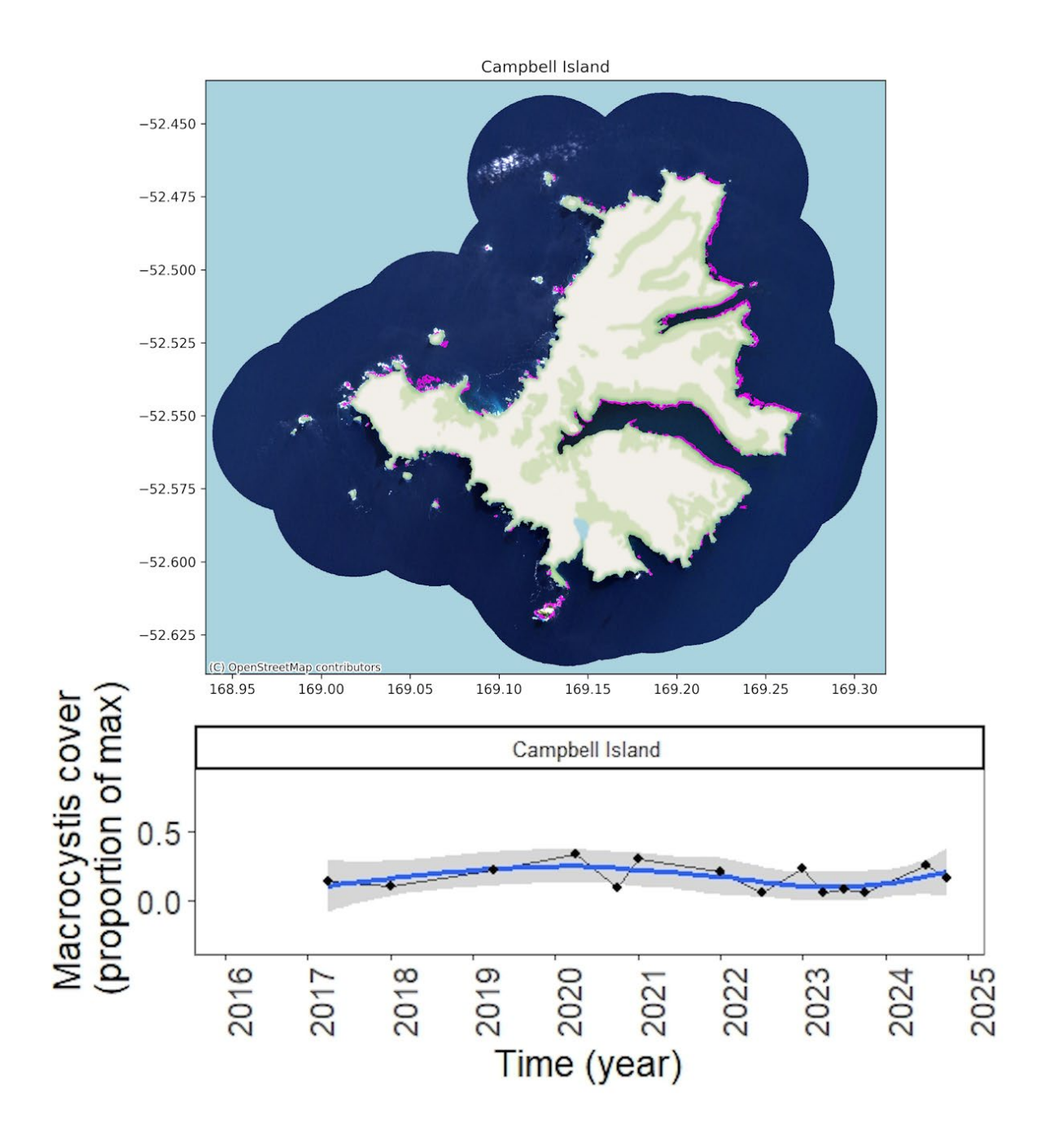


Figure 20: Combined distribution of kelp over the 10-year timeseries of Sentinel-2 imagery for Campbell Island. Map shows the area clipped for processing, including the removal of land and constant buffer around coastlines. Purple polygons show kelp detected. Bottom figure shows the coverage of kelp over time, presented as a proportion of the maximum coverage detected across the timeseries.

3.2 Environmental drivers of kelp abundance

The influence of two key environmental parameters on kelp distribution were examined, sea surface temperature and water clarity. *Macrocystis* occurs across a wide latitudinal range, and therefore, lives across a diverse range of temperatures. There have been, however, major SST anomalies over the past twenty years (Figure 21). Temperatures across the New Zealand EEZ were elevated for multiple years from about 2018 to 2020, and again from 2022 to 2024, with a notable summer peak in temperatures in 2023. When visualised alongside the trends in proportional cover of *Macrocystis* there was correlation between periods of high temperatures (both prolonged periods of elevated SST – Figure 21 - and spikes in SST) and troughs in cover of *Macrocystis* across the full geographic range (Figure 22). However, this is somewhat masked by the fact that this data spans the full geographic range of New Zealand (i.e., data is simultaneously showing *Macrocystis* cover in areas where temperatures are both above and below thermal thresholds). There were multiple instances across sites when the SST threshold of 19 °C was exceeded, and all sites except the sub-Antarctic Islands experienced an exceedance of the lower temperature threshold of 17 °C (an indication that the sites may be impacted under climate change scenarios.

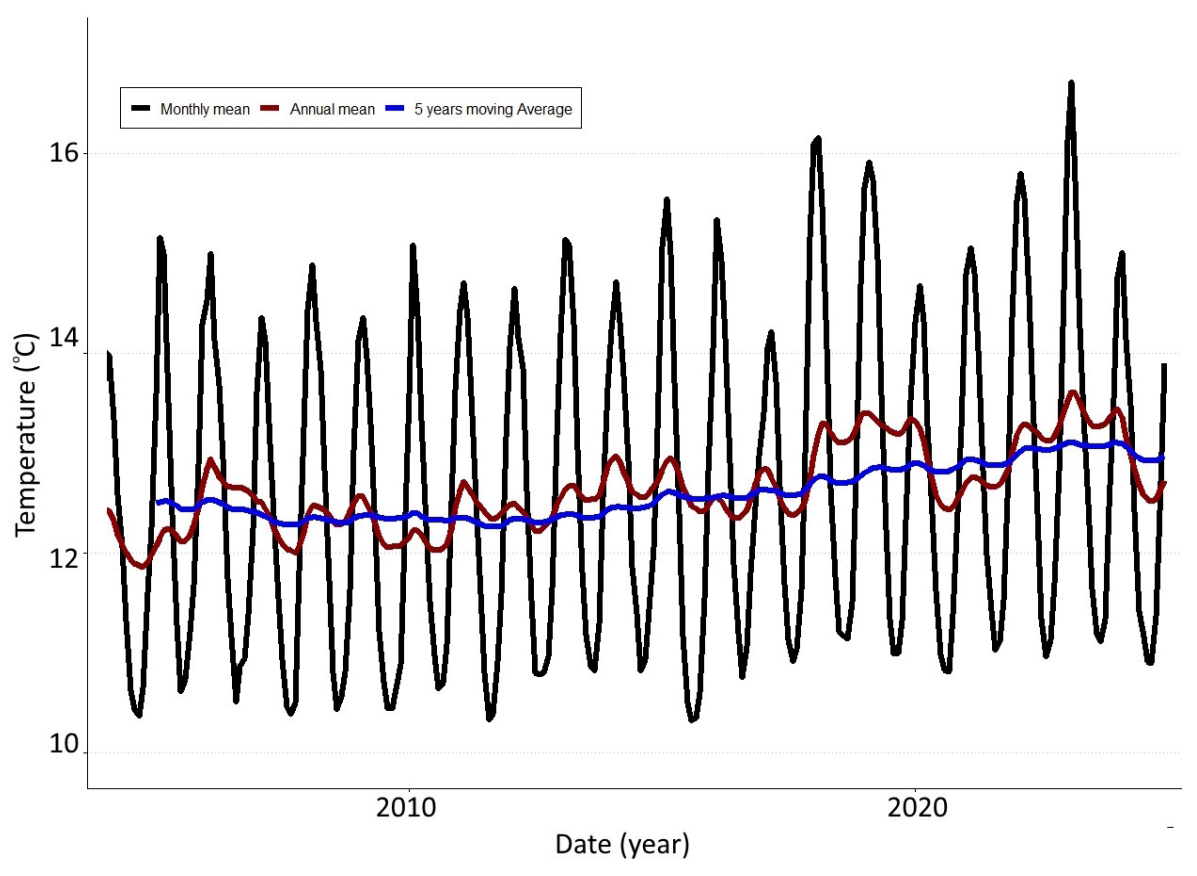


Figure 21: Mean Sea Surface Temperature (SST) across New Zealand EEZ over the past 20 years (2005–2025, data from NOAA Optimum Interpolation Sea Surface Temperature dataset). Temperature presented as monthly means (black), annual mean (red) and 5 year moving mean (blue).

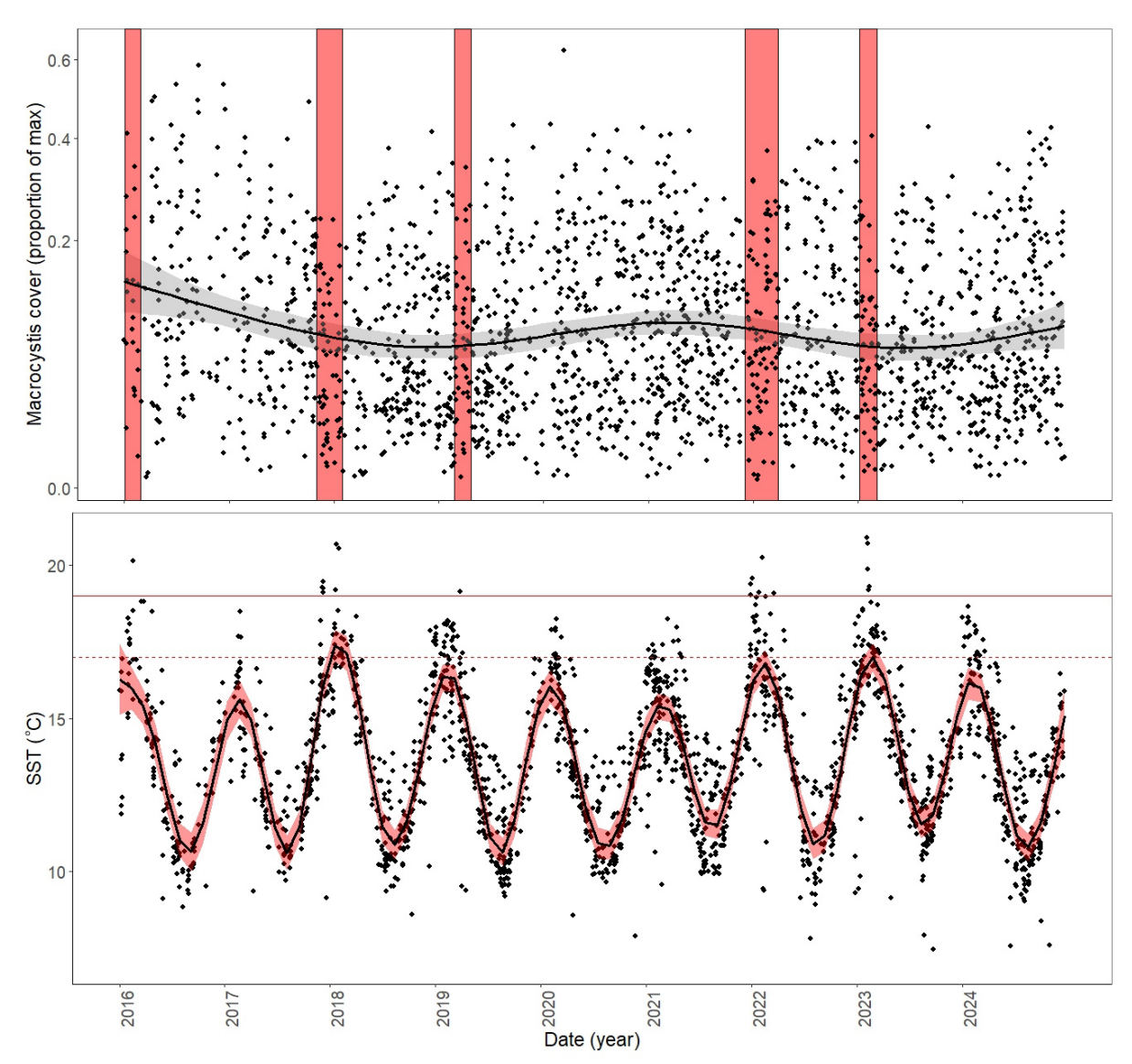


Figure 22: Proportional cover of *Macrocystis* across New Zealand (top) and associated Sea Surface Temperature at the locations analysed (bottom). Trendlines fitted by General Additive Models (GAM), including 95% confidence intervals. Data presented from 2015–2025. Each data point represents *Macrocystis* cover (as a proportion of maximum) for each site for each available satellite pass. Red shaded boxes indicate periods where SST over 19 °C were observed at one or more of the focal areas. Horizontal lines indicate key SST thresholds of 19 °C (solid red line), and 17°C (dashed red line).

Regional breakdown of the trends between *Macrocystis* cover and SST show greater detail in the regions experiencing the highest temperatures and the strongest declines in *Macrocystis* cover. The Wellington region had five SST events exceeding 19 °C, many of which were associated with periods of low *Macrocystis* cover (Figure 23). The long-term SST trend showed that periods of elevated SST were associated with short-term values of low kelp cover. The lower threshold of 17 °C was regularly crossed each year. In general, the Wellington region had low proportional cover of *Macrocystis*, and periods of high SST were associated with further declines in cover.

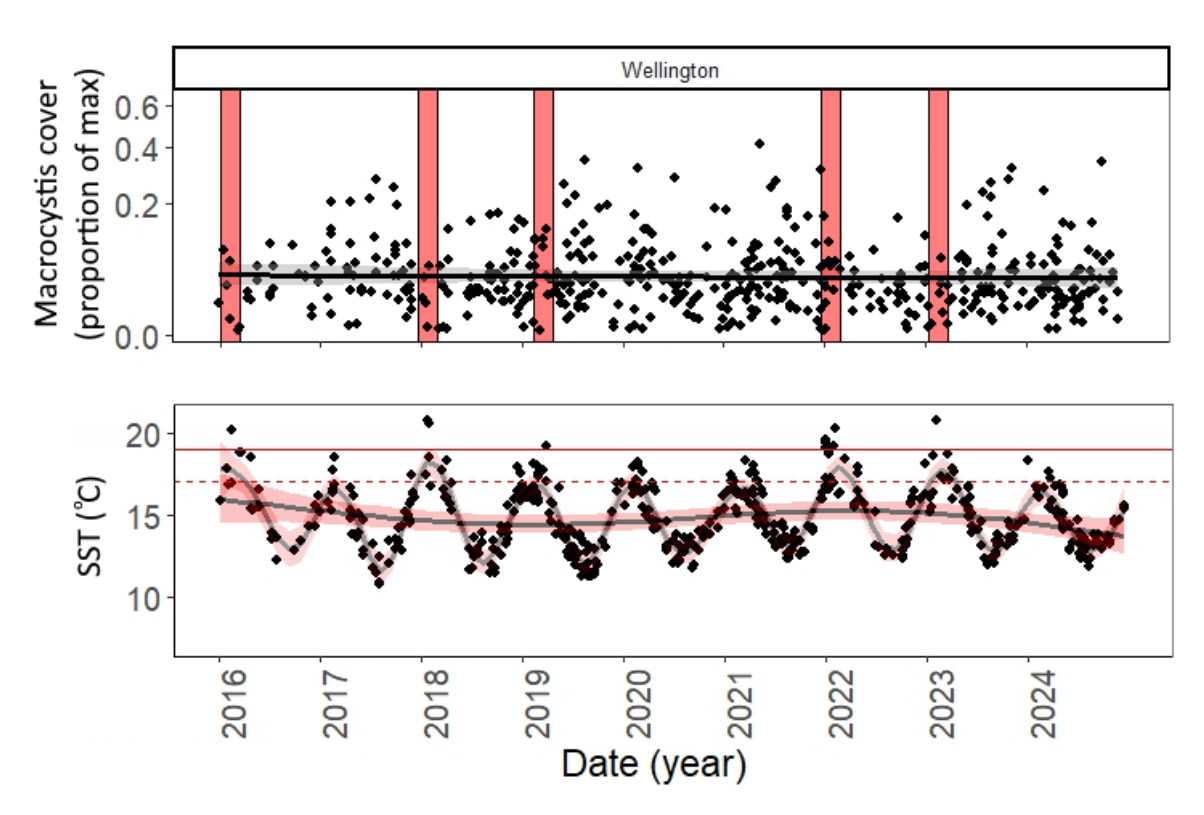


Figure 23: Proportional cover of *Macrocystis* for the Wellington region, including Porirua, Wellington, and the Marlborough Sounds (top) and associated Sea Surface Temperature at the locations analysed (bottom). Trendlines fitted by General Additive Models (GAM), including 95% confidence intervals. For SST, two GAM trendline models are plotted, one complex model showing seasonal models, and a second showing longer trends. Data presented from 2015–2025. Each data point represents *Macrocystis* cover (as a proportion of maximum) for each site (e.g., Porirua, Marlborough etc) for each available satellite pass. Red shaded boxes indicate periods where SST over 19°C were observed at one or more of the focal areas. Horizontal lines indicate key SST thresholds of 19°C (solid red line), and 17°C (dashed red line).

The Canterbury region had three events exceeding 19 °C, all of which were associated with declines in *Macrocystis* cover (Figure 24). *Macrocystis* cover declined during periods of elevated temperature, with the proportional cover and SST trendlines showing the inverse response. The lower threshold of 17 °C was regularly crossed each year. The Canterbury region had moderate proportional cover of *Macrocystis*..

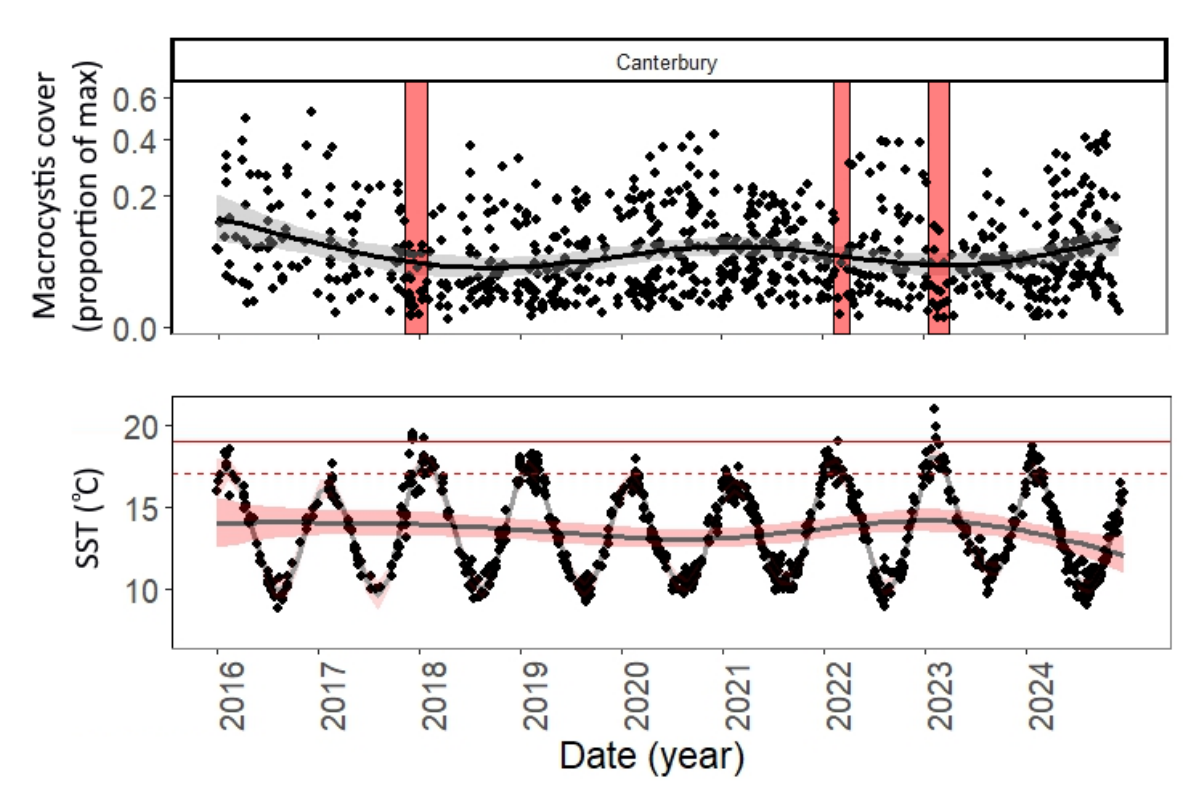


Figure 24: Proportional cover of *Macrocystis* for the Canterbury region, including Wharanui, Motunau, Diamond Harbour, Akaroa, and Timaru (top) and associated Sea Surface Temperature at the locations analysed (bottom). Trendlines fitted by General Additive Models (GAM), including 95% confidence intervals. For SST, two GAM trendline models are plotted, one complex model showing seasonal models, and a second showing longer trends. Data presented from 2015–2025. Each data point represents *Macrocystis* cover (as a proportion of maximum) for each site (e.g., Motunau, Timaru) for each available satellite pass. Red shaded boxes indicate periods where SST over 19 °C were observed at one or more of the focal areas. Horizontal lines indicate key SST thresholds of 19 °C (solid red line), and 17°C (dashed red line).

Chatham Island had no SST events exceeding 19 °C and only two events exceeding 17 °C (Figure 25). Lower mean temperatures early in the 10-year time series were associated with high proportional cover of *Macrocystis*, while proportional cover at these sites declined over time as average temperatures increased. In this case, the switch from relatively high proportional cover values to relatively low proportional cover represents a potential major shift in the occupation of rocky reef areas by *Macrocystis*.

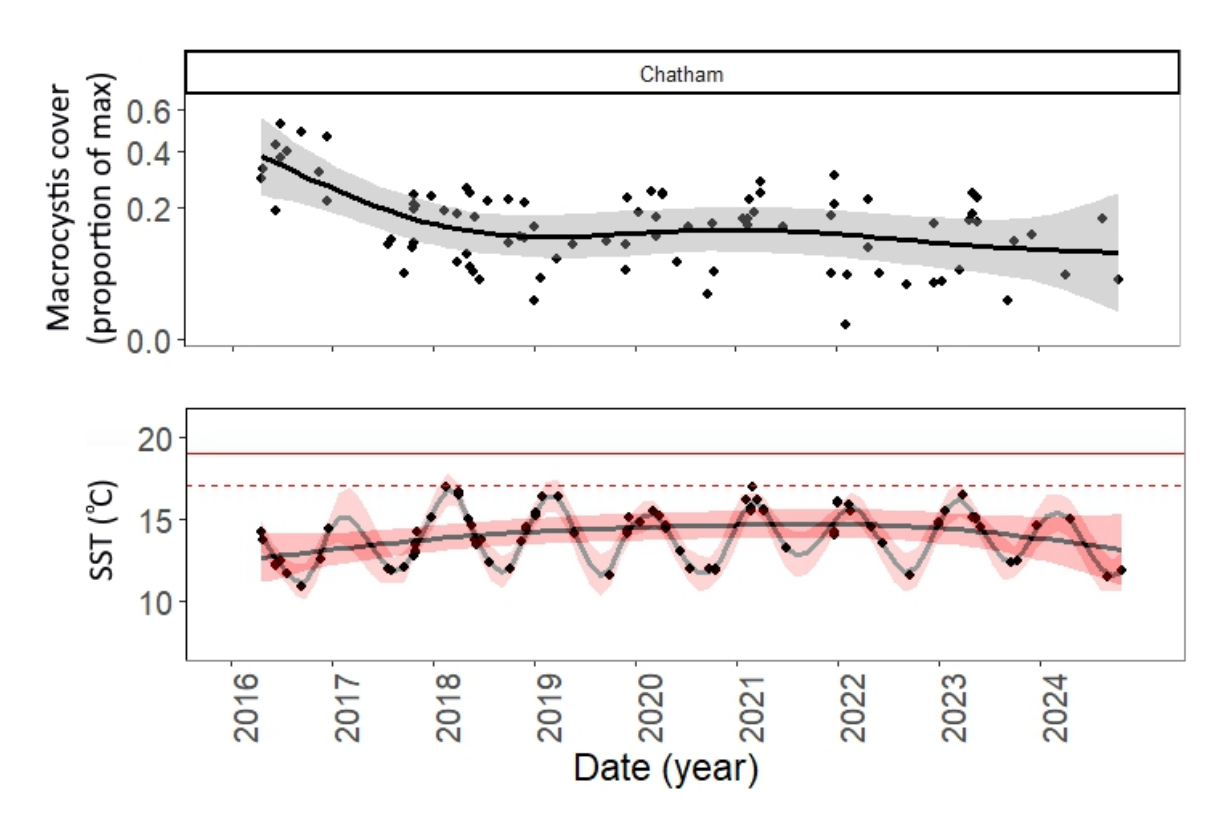


Figure 25: Proportional cover of *Macrocystis* for the Chatham region, including Chatham and Pitt Islands (top) and associated Sea Surface Temperature at the locations analysed (bottom). Trendlines fitted by General Additive Models (GAM), including 95% confidence intervals. Data presented from 2015–2025. Each data point represents *Macrocystis* cover (as a proportion of maximum) for each site (e.g., Chatham Island) for each available satellite pass. For SST, two GAM trendline models are plotted, one complex model showing seasonal models, and a second showing longer trends. Horizontal lines indicate key SST thresholds of 19 °C (solid red line), and 17 °C (dashed red line).

The Otago region had no SST events exceeding 19 °C and few events exceeding 17 °C (Figure 26). However, there was an inverse relationship between the longer-term trend of SST and proportional kelp cover. In general, the Otago region had moderate to high proportional cover throughout the ten-year time series, however, the largest increase in SST was coincident with a brief period of low kelp cover.

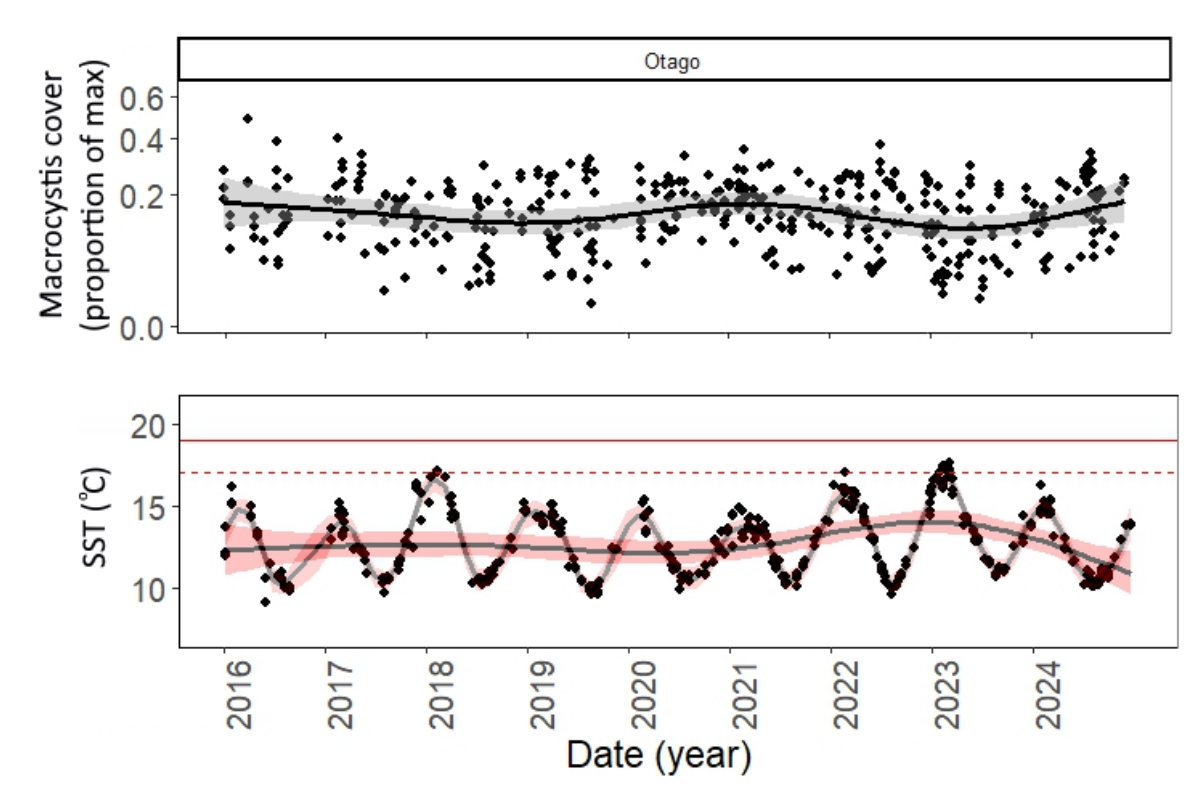


Figure 26: Proportional cover of *Macrocystis* for the Otago region, including Waikouaiti and Otekura (top) and associated Sea Surface Temperature at the locations analysed (bottom). Trendlines fitted by General Additive Models (GAM), including 95% confidence intervals. Data presented from 2015–2025. Each data point represents *Macrocystis* cover (as a proportion of maximum) for each site (e.g., Waikouaiti) for each available satellite pass. For SST, two GAM trendline models are plotted, one complex model showing seasonal models, and a second showing longer trends. Horizontal lines indicate key SST thresholds of 19°C (solid red line), and 17°C (dashed red line).

The Southland region had two events exceeding 19 °C and few events exceeding 17 °C (Figure 27). Both events were associated with a temporary decline in *Macrocystis* cover, and there was an indication of an inverse relationship between proportional cover and SST. The summers of 2022 and 2023 had SST values just exceeding 19 °C and coincided with notably low proportional cover of *Macrocystis*. Likewise exceedance of 17 °C in 2018 was also associated with low cover of *Macrocystis*.

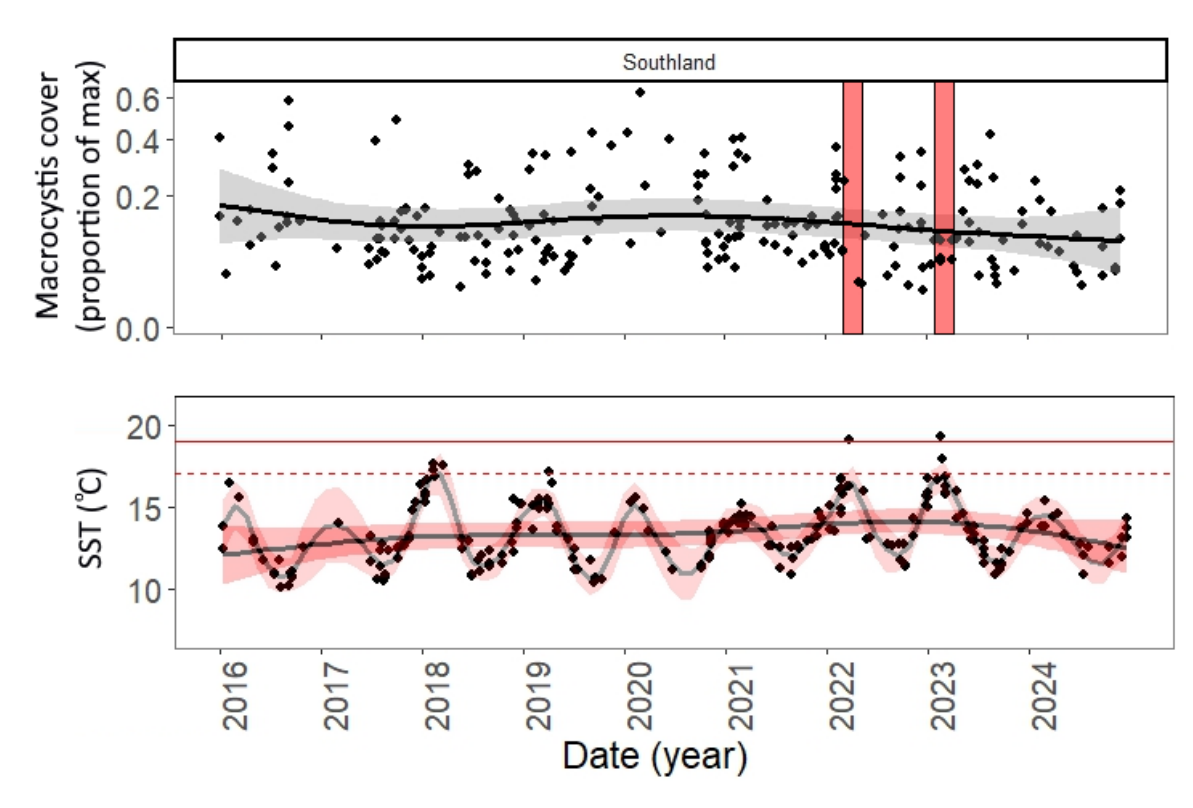


Figure 27: Proportional cover of *Macrocystis* for the Southland region, including Breaksea Sound, Long Sound, Bluff, Rakiura, and Pearl Island, (top) and associated Sea Surface Temperature at the locations analysed (bottom). Trendlines fitted by General Additive Models (GAM), including 95% confidence intervals. For SST, two GAM trendline models are plotted, one complex model showing seasonal models, and a second showing longer trends. Data presented from 2015–2025. Each data point represents *Macrocystis* cover (as a proportion of maximum) for each site (e.g., Bluff, Rakiura) for each available satellite pass. Red shaded boxes indicate periods where SST over 19°C were observed at one or more of the focal areas. Horizontal lines indicate key SST thresholds of 19°C (solid red line), and 17 °C (dashed red line).

The sub-Antarctic region has a lower temperature regime than mainland New Zealand with SST rarely exceeding 12 °C (Figure 28). Unlike other regions, the sub-Antarctic region has higher proportional cover during warmer conditions. However, the limited availability of quality satellite passes for this region impacts the ability to interpret the influence of SST of *Macrocystis* cover.

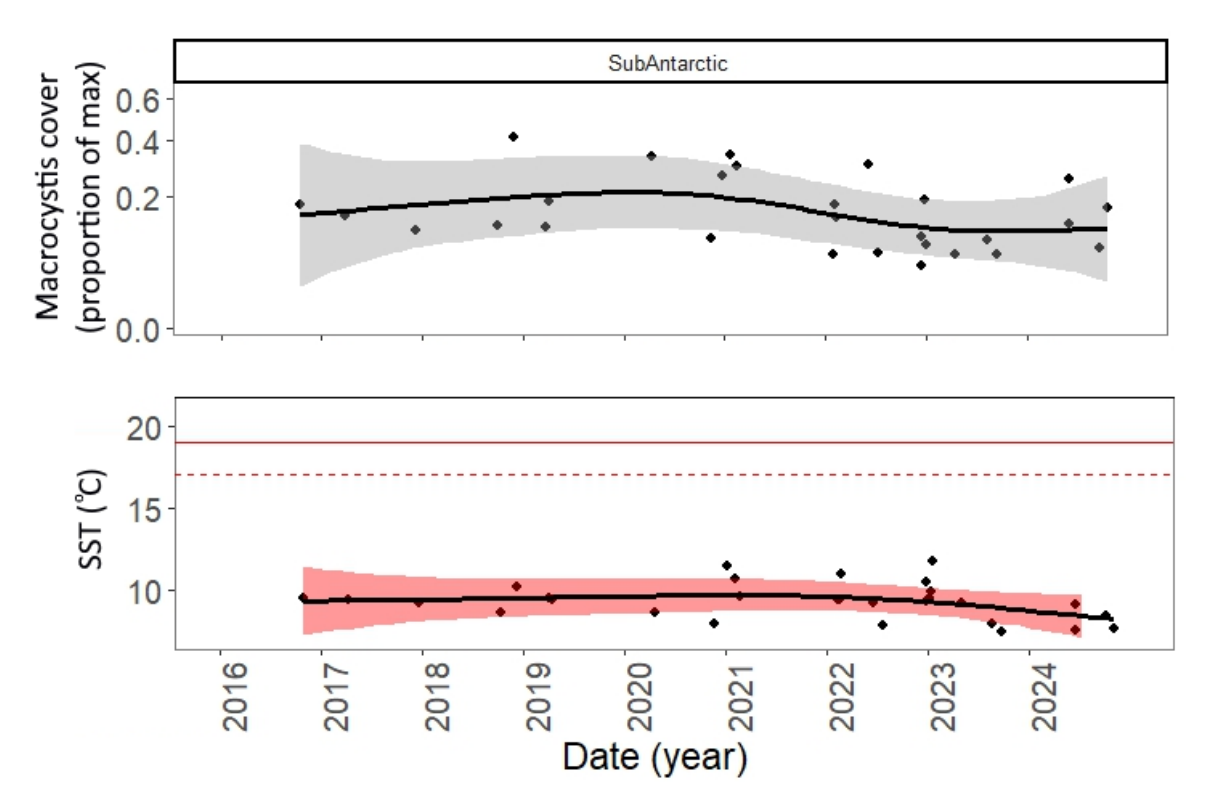


Figure 28: Proportional cover of *Macrocystis* for the Sub-Antarctic region, including Auckland and Campbell Islands (top) and associated Sea Surface Temperature at the locations analysed (bottom). Trendlines fitted by General Additive Models (GAM), including 95% confidence intervals. Data presented from 2015–2025. Each data point represents *Macrocystis* cover (as a proportion of maximum) for each site (e.g., Auckland Island) for each available satellite pass. Horizontal lines indicate key SST thresholds of 19 °C (solid red line), and 17 °C (dashed red line).

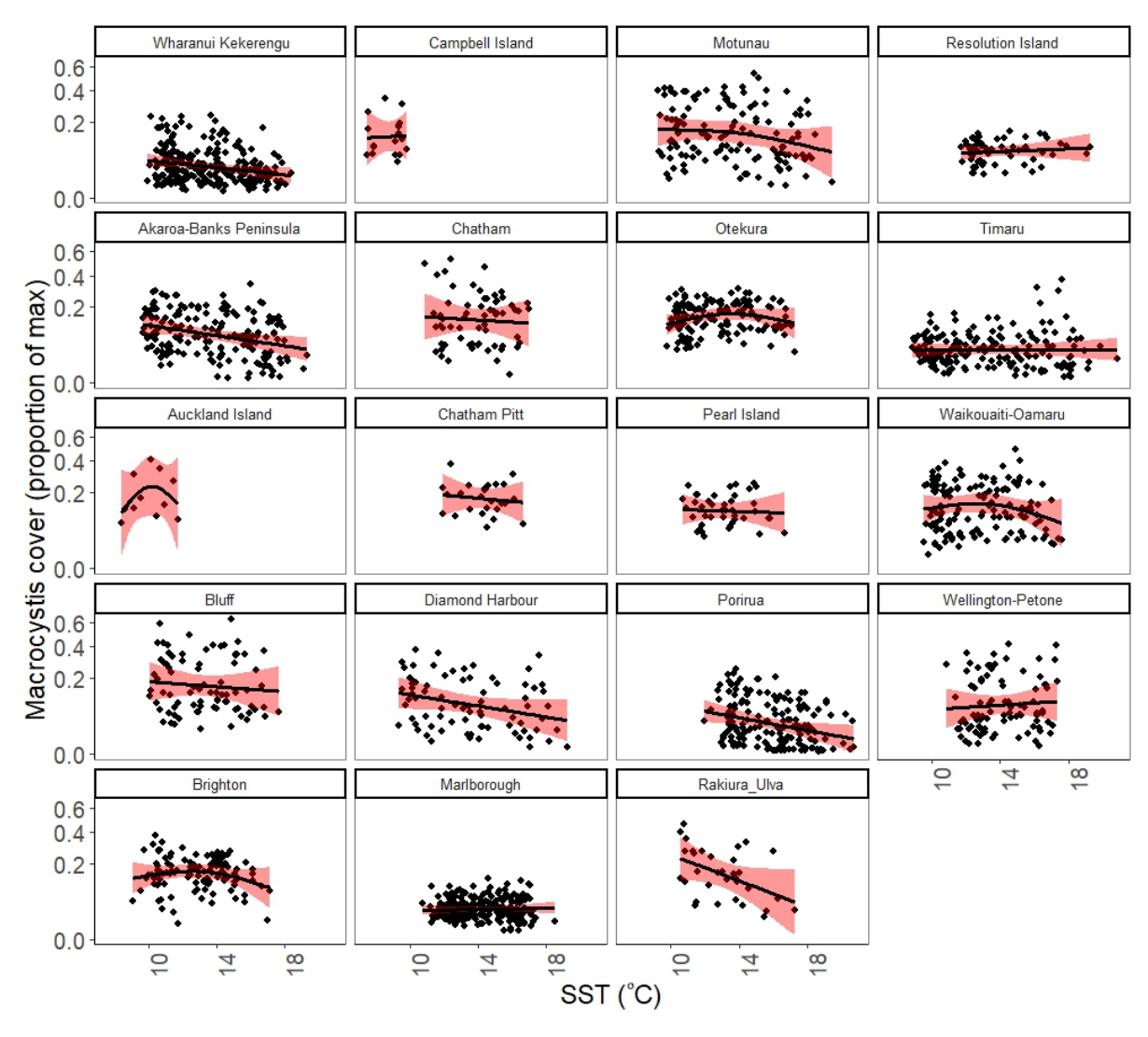


Figure 29: Proportional cover of *Macrocystis* against Sea Surface Temperature (SST) for each site. Trendlines fitted by General Additive Models (GAM), including 95% confidence intervals. Each data point represents *Macrocystis* cover (as a proportion of maximum) for each available satellite pass.

Table 1: General Additive Model analysis for the main effects of Sea Surface Temperature (SST) on kelp cover across sites. Significant results shown by bold and italics and by symbols (*** p < 0.001, ** p < 0.01, * p < 0.05, . = p < 0.1.

Site	edf	df	F	p-value	Significance
Wharanui - Kekerengu	7.8	9	13.5	< 2e-16	***
Akaroa - Banks Peninsula	0.0001	9	0	0.9	
Auckland Island - Island	1.2	8	0.6	0.03	*
Bluff	<i>7.3</i>	9	7.8	< 2e-16	***
Campbell Island - Island	0.0002	6	0	0.7	
Chatham	2.5	9	1.3	0.002162	**
Chatham Pitt - Pitt	2.3	9	1.8	0.0002	***
Diamond Harbour - Harbour	0.0002	9	0	0.741492	
Marlborough	6.2	9	15.2	< 2e-16	***
Motunau	0.0001	9	0	0.8	
Pearl Island - Island	0.0002	9	0	0.6	
Porirua	2.9	9	3.2	5.07E-07	***
Rakiura_Ulva - Ulva	0.9	9	1.3	0.0004	***
Resolution Island - Island	1.3	9	0.3	0.09	
Timaru	2.6	9	4.4	< 2e-16	***
Waikouaiti-Oamaru - Oamaru	3.9	9	2.4	9.60E-05	***
Wellington - Petone	0.8	9	0.4	0.03	*

When proportional cover of *Macrocystis* was plotted SST for each site (Figure 29), declines in kelp cover at seen at high temperatures across regions. Analysis of individual sites showed that Wharanui/Kekerengu, Auckland Island, Bluff, Chatham Islands, Marlborough, Porirua, Rakiura, Timaru, and Wellington all had a significant relationship between SST and kelp cover (Table 1). However, results were only weakly significant for Auckland Island and Wellington.

The relationship between *Macrocystis* cover and SST across all sites showed a strong trend of declining cover (both m² and proportion of maximum cover) with increasing temperature (Figure 30). Reduced cover of *Macrocystis* was particularly evident beyond the lower threshold of 17 °C. The relationship has the same general shape for both the area covered (m²) and proportional coverage of *Macrocystis*. Water clarity (i.e., the attenuation coefficient Kd) had less influence on the cover (m² and proportional) of *Macrocystis*, but there was a general trend of declining cover with increasing clarity (Figure 31).

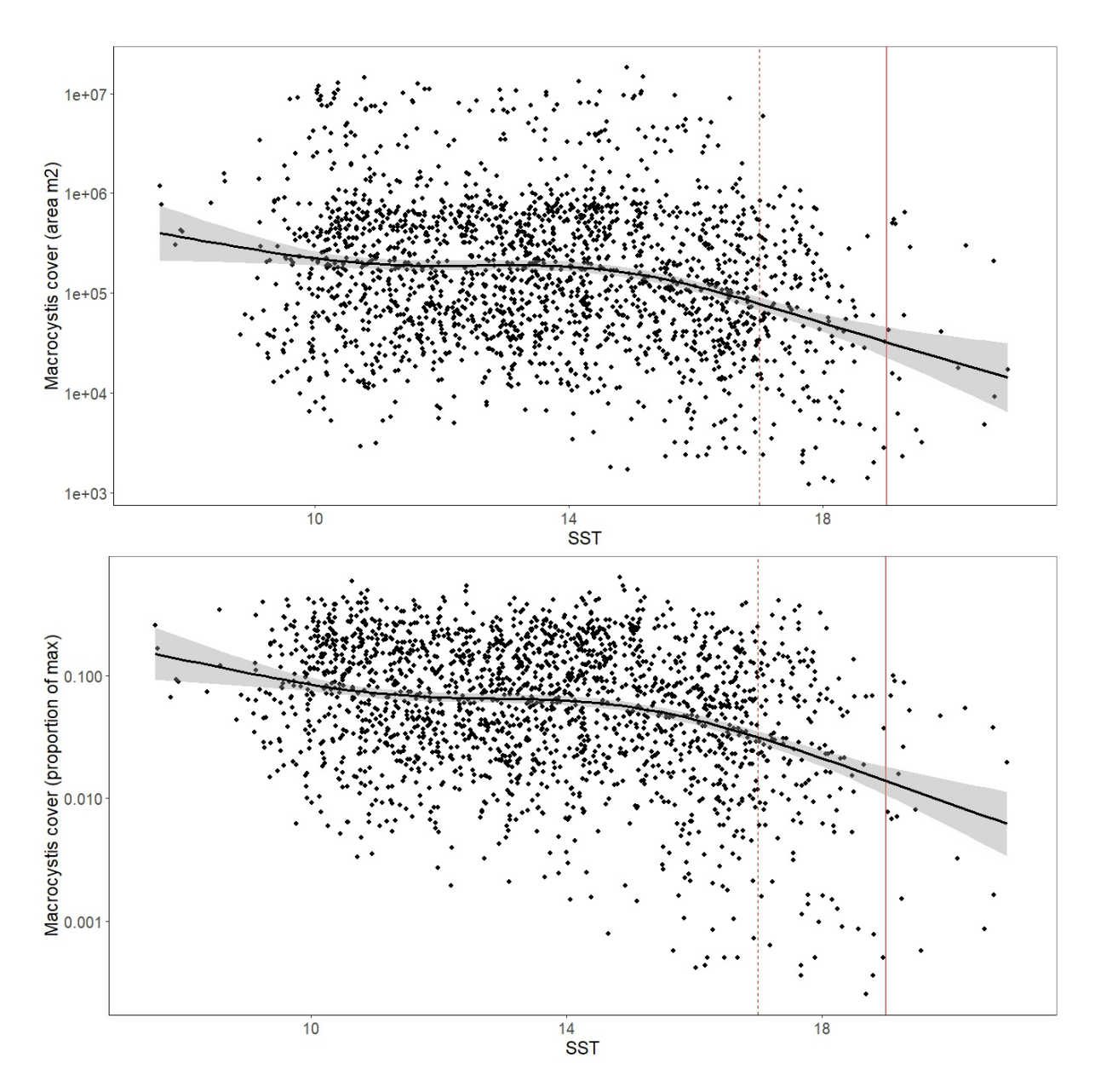


Figure 30: Relationship between the cover of *Macrocystis* and Sea Surface Temperature (SST) across all sites and times. Top plot shows *Macrocystis* cover defined by area (m²) on a log scale, and the bottom plot shows *Macrocystis* cover as a proportion of the maximum cover on a log scale. Trendlines fitted by General Additive Models (GAM), including 95% confidence intervals. Vertical lines indicate key SST thresholds of 19 °C (solid red line), and 17 °C (dashed red line).

Analyses showed that SST had a significant effect on *Macrocystis* cover and there was a weak trend of declining kelp with reduced water clarity (Table 2). When visualised, these analyses showed that there was a combined negative effect of increasing SST and decreasing water clarity (increasing Kd values) (Figure 32). SST over 15–16 °C were associated with the inflection in the fitted curve for *Macrocystis* cover.

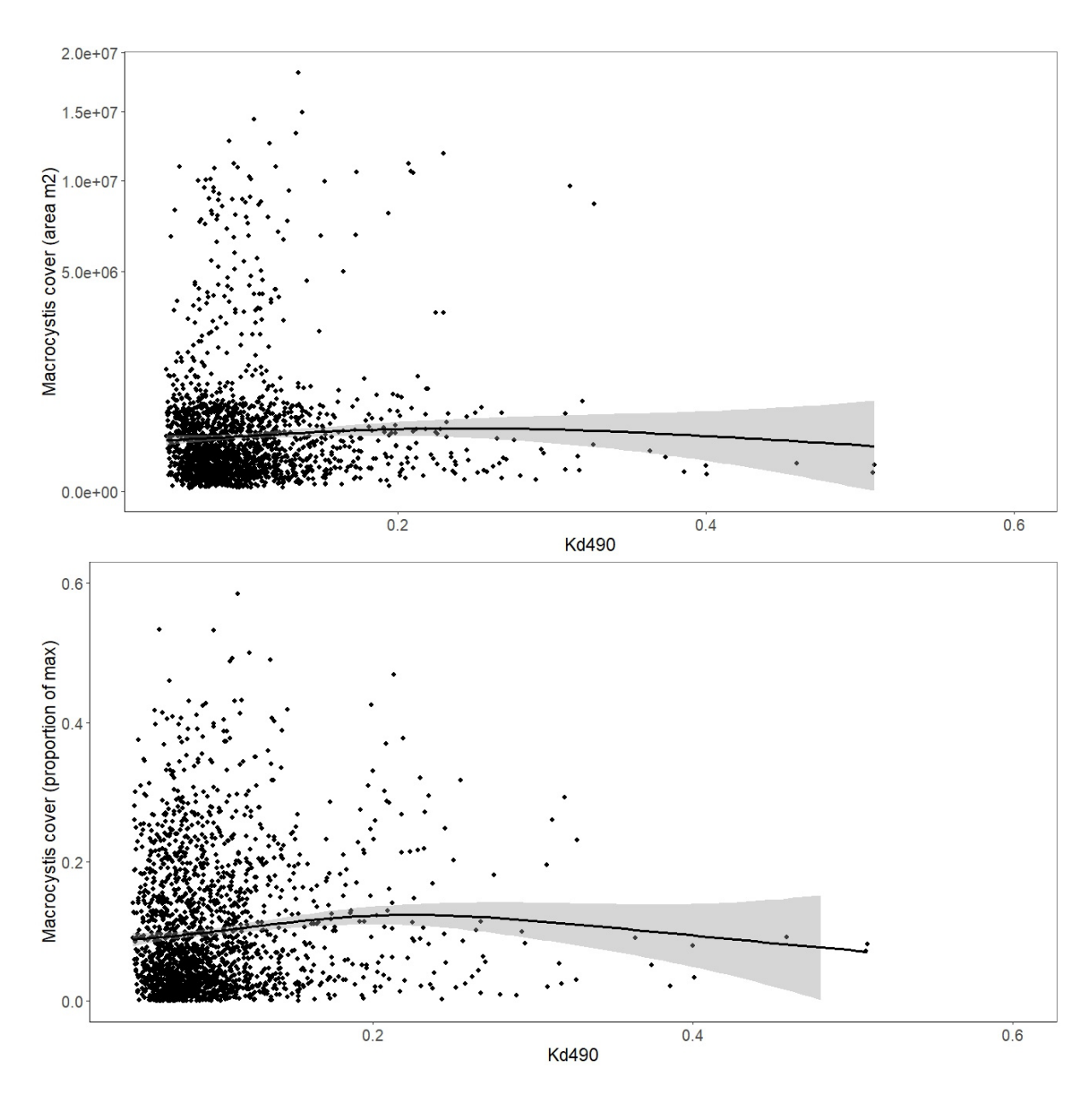


Figure 31: Relationship between the cover of *Macrocystis* and light attenuation (Kd490) across all sites and times. Top plot shows *Macrocystis* cover defined by area (m²) square root transformed, and the bottom plot shows *Macrocystis* cover as a proportion of the maximum cover (no transformation). Trendlines fitted by General Additive Models (GAM), including 95% confidence intervals.

Table 2: General Additive Model analysis for the main effects of Sea Surface Temperature (SST) and water clarity (Kd).

Parameters	edf	df	F	p-value
SST Kd	4.4 1.4	9 9	5.6 0.4	<0.001 0.060
R-sq Deviance explained	0.65 75%			
n	1 794			

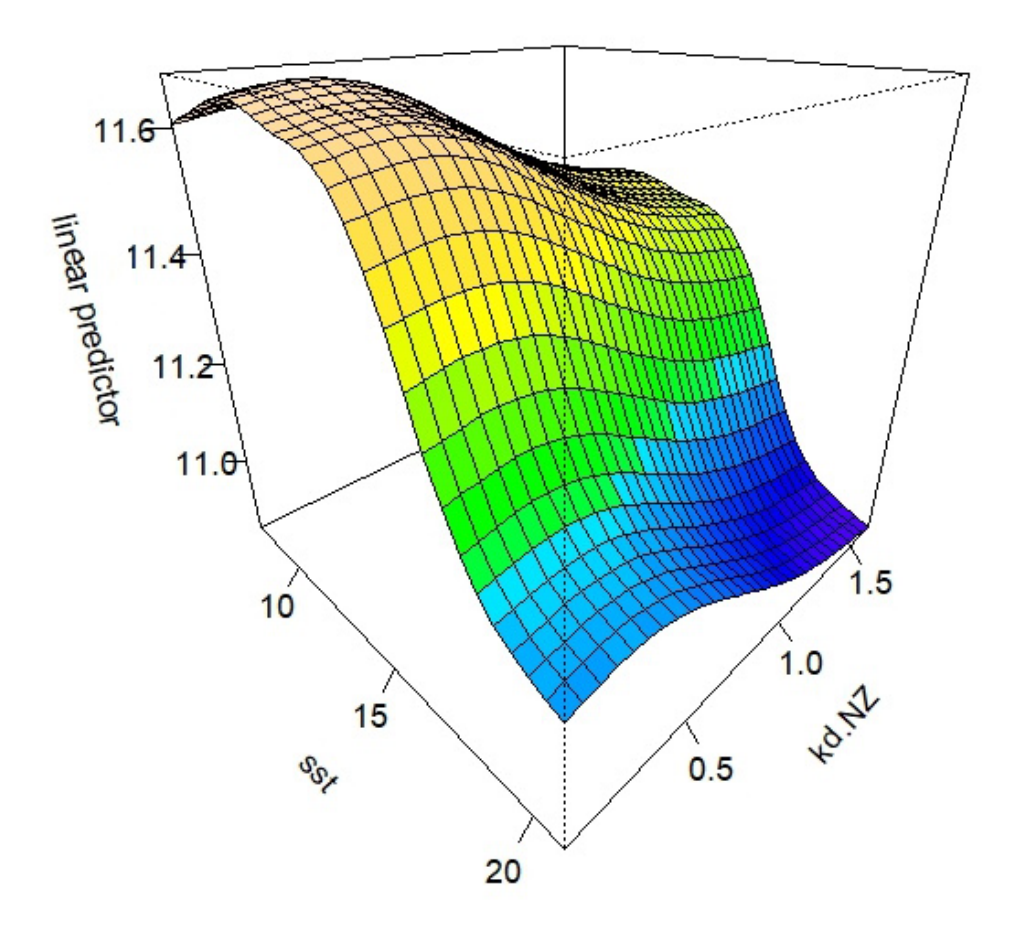


Figure 32: Three-dimensional plot showing the General Additive Model (GAM) analysis of the influence of SST and Kd on cover of *Macrocystis* (linear predictor).

4 DISCUSSION

Giant kelp, *Macrocystis pyrifera*, is one of earth's fastest growing photosynthetic organisms, and is a key contributor to carbon fixation and habitat provision for temperate marine ecosystems across a large extent of the world's temperate coastlines (Schiel & Foster 2015; Miller et al. 2018). Synthesis of long-term observations using satellite remote sensing have enabled analyses of broad scale processes relating to oceanographic trends (Cavanaugh et al. 2011; Hamilton et al. 2020), and these methods have equal promise for better understanding the point-source and diffuse influences of land-use changes on kelp forests (Tait et al. 2021).

Satellite remote sensing is increasingly being used to map and monitor kelp beds (Cavanaugh et al. 2011, Bell et al. 2020; Mora-Soto et al. 2020, Tait et al. 2021). It presents a cost-effective option for a variety of management purposes and provides decadal scale observations across broad biogeographic zones (Huovinen et al. 2020; Hamilton et al. 2020). We note, however, that there are a variety of challenges to applying automated algorithms for the detection and delimitation of kelp forests. In particular, extraction of quality imagery for the sub-Antarctic Islands (Auckland and Campbell Islands at 50° and 52° latitude) was sporadic and impacted by poor light and high cloud cover. Furthermore, we acknowledge that the polygons used covered very large areas of coastline and as result produce a range of false detections. These false detections appear to be related to various types of aquatic vegetation, including:

• Rocky reef macroalgae, particularly *Carpophyllum* spp, *Durvillaea* spp.

- Estuarine macroalgae
- Beach cast and drifting macroalgae

This approach has been used purposefully to identify areas that aren't necessarily identified in formal records. We note a particular bed near Mana Island (Porirua) and the Wharanui-Kekerengu Reef near Kaikōura. Further work can focus in on key regions and better quantify cover through time and support *in situ* site selection. For example, some sites may require a small amount of in situ validation, while other sites could be further explored using remote sensing, but targeting more discrete areas of interest.

Regional trends

We identify generally consistent coverage of *Macrocystis* through time, although locations can vary greatly in the capacity for *Macrocystis* beds. Regions with the most extensive kelp forests include the Otago Region (Waikouaiti-Oamaru), the Chatham Islands, Campbell Island, Auckland Island, Rakiura, and Akaroa. Even amongst these areas there were some areas with declining trends.

- **Timaru** had a notable trend of decline through time. In the early parts of the time series (2015–2017) there were some high values of *Macrocystis* cover but large declines occurred from 2018–2025.
- Rakiura is one of the regions with the largest combined kelp cover. Since 2022 cover has been low and sporadic. The Southland region has seen some notably high SST values, especially considering the Chathams or Otago regions (at higher latitudes) rarely had mean monthly temperatures above 17 °C, while Southland twice had values over 19 °C.
- **Porirua** The kelp beds in the Porirua region are substantial but can be low at times. A strong decline in kelp cover with increasing SST was evident (Figure 29; Table 1). Further work should examine the potential for false detections in the region and characterise different macroalgal groups.
- Wharanui-Kekerengu The Wharanui- Kekerengu region had, at times, high cover of *Macrocystis*, but also had long periods of very low cover, and at times the core offshore beds were completely absent. Timeseries shows strong correlation with SST and this region is closer to the upper end of the temperature threshold for *Macrocystis* (Figure 29; Table 1).

Additionally, areas that require watching or further analysis/study due to their sensitivity, importance and a national level, or exposure to climatic events include:

- **Bluff** The Bluff region had variability in kelp forest cover over time and shows signs of decline from 2023 onwards. Errors introduced from other macroalgal beds further in Bluff Harbour may contribute to this trend. Further inspection, in situ sampling, and analysis are required.
- Chathams were initially one of the regions with the greatest kelp cover, but from 2018–2025 there was a large and sustained decline in kelp.
- Long Sound Long Sound showed signs of decline over time, especially since 2023. However, regions in the upper Fiord are contributing to high numbers in some samples. Confirmation that these are kelp rather than other macroalgae, or errors associated with shading from the Fiords would be required.
- Otago The Otago region has the largest kelp beds and is relatively stable through time. There are, however, indications that kelp cover is responding to broad trends in SST. The region has both the largest and most persistent beds across the whole of our EEZ and shows negative responses to high SST.
- Marlborough There was a significant influence of SST on kelp cover in Marlborough. Furthermore, the very low coverage in this region suggested that Macrocystis was limited in its abundance and consistency through time.

Environmental drivers

New Zealand has experienced some of the most intense marine heat waves on record in the past 5 years (Salinger et al. 2019; Salinger et al. 2020) causing localised losses of southern bull kelp (Thomsen et al. 2019) and *Macrocystis* (Tait et al. 2021). Rapid rates of land-use change associated with agriculture and urbanisation have greatly altered the land-water interface globally, including in New Zealand, where rates of sedimentation have also increased (Goff 1997). The proximity of *Macrocystis* forests in the nearshore zone to sources of sediments greatly affects the demography of populations of large brown algae that are the facilitators of diversity and energy flow in nearshore waters. Sediments may prevent attachment of algal propagules to benthic surfaces (Taylor & Schiel 2003: Schiel et al. 2006), smother those that have settled (Schiel & Gunn 2019), and result in a poor conversion from juvenile *Macrocystis* sporophytes to adult plants reaching the surface (Tait 2019).

Declines in *Macrocystis* have been ascribed to anomalous warm events and sedimentation, but other mechanisms for kelp loss include altered trophic interactions and destructive grazing by urchins (Ling et al. 2009; Rogers-Bennett & Catton 2019; Butler et al. 2020) and nutrient limitation (Dean & Jacobson 1986; Hernandez-Carmona et al. 2001; Edwards & Hernandez-Carmona 2005; McPherson et al. 2021).

In this study mean monthly SST values above about 17°C were associated with a notable decline in kelp cover across sites, while values greater than 19°C were associated with very low kelp cover. In most cases, kelp forest cover rebounded within 3–6 months of SST correlated declines. There was no clear association between turbidity and kelp cover.

This research shows that the abundance and cover of *Macrocystis* is particularly constrained at the northern limits of its distribution, where it is subject to significant variability, tightly linked to SST. Furthermore, one of the regions with the highest turbidity (i.e., Timaru) also had notable declines in kelp cover through time. As described above in the regional trends, we identified several regions where there is a strong correlation between high SST and low *Macrocystis* cover. In particular, Wharanui-Kekerengu, Bluff, Marlborough, Porirua, Timaru, Chatham Island, Rakiura, and Otago show strong responses to high SST (Figure 29; Table 1).

5 POTENTIAL RESEARCH

This study has enabled large regions of New Zealand's coastline to be explored for the presence of offshore *Macrocystis* beds. It has, in fact, turned up key data on several beds for which few records exist, particularly those on Mana Bridge (Porirua), and off the northern Kaikōura coast (Wharanui-Kekerengu). However, as identified earlier, some areas of false positives exist. Further research could refine the target areas to focus on the key areas of *Macrocystis* and further investigate areas of uncertainty or concern. These include:

- 1. Long Sound in Fiordland had detections which suggested large *Macrocystis* beds further in the sound. However, these may be erroneous detections and require field validation.
- 2. There has been a potential major decline in *Macrocystis* at the Chatham Islands. While this is correlated to higher-than-average temperatures, the values do not exceed any major thresholds. Additional work, such as further interrogation of the satellite data and ancillary datasets (e.g., satellite derived water quality, or wave action) or in situ validation, to understand these trends may be required to assess the validity and potential underlying causes.
- 3. High temperatures in Southland and erratic trends in *Macrocystis* beds also may suggest that these beds are particularly vulnerable. Additional interrogation of satellite datasets, particularly of water quality parameters, may be required to understand if management actions (e.g., land-to-sea catchment management) may provide resilience to vulnerable kelp beds.

6 FULFILMENT OF BROADER OUTCOMES

As required under Government Procurement rules², Fisheries New Zealand considered broader outcomes (secondary benefits such as environmental, social, economic or cultural benefits) that would be generated by this project. The primary outcome of this research was to understand the trends and distribution of *Macrocystis* across New Zealand as a way of assessing the health of the fishery for kelp, and reliant fisheries. However, this research provides broader outcomes, especially with respect to the monitoring of ecological impacts of climate change and extreme events. The continuous passive monitoring of *Macrocystis* through remote sensing provides a cheap and effective tool for understanding how events have impacted a key ecosystem engineer over broad biogeographic gradients.

This research and the online tool we provide will be able to inform agencies from MPI (Fisheries New Zealand) to local and regional councils about trends of macroalgal populations and allow the inference of broad ecological impacts of climatic events. Furthermore, few spatially explicit timeseries for kelp exist for the sub-Antarctic Islands. The research here shows that satellite remote sensing can be successfully applied to southernmost portion of New Zealand's EEZ and could inform the conservation of these ecologically significant islands.

² https://www.procurement.govt.nz/procurement/principles-charter-and-rules/government-procurement-rules/planning-your-procurement/broader-outcomes/

7 ACKNOWLEDGEMENTS

This report was funded by Fisheries New Zealand project ZBD202305. We acknowledge the contribution of Ministry for Primary Industries staff for their assistance in developing the research. In particular, we thank Dr Jean Davis for her leadership and guidance. We also thank Marjan van den Belt for helping establish and develop the research project. We thank Darren Parsons and Richard O'Driscoll for their constructive reviews of this report.

8 REFERENCES

- Airoldi, L. (2003). The effects of sedimentation on rocky coast assemblages. *Oceanography and Marine Biology*, *41*, 169–171.
- Alestra, T.; Tait, L.W.; Schiel, D.R. (2014). Effects of algal turfs and sediment accumulation on replenishment and primary productivity of fucoid assemblages. *Marine Ecology Progress Series*, 511, 59–70.
- Arafeh-Dalmau, N.; Montaño-Moctezuma, G.; Martinez, J.A.; Beas-Luna, R.; Schoeman, D.S.; Torres-Moye, G. (2019). Extreme marine heatwaves alter kelp forest community near its equatorward distribution limit. *Frontiers of Marine Science* 6:499. doi: 10.3389/fmars.2019.00499
- Arakawa, H.; Matsuike, K. (1992). Influence on insertion of zoospores germination survival and maturation of gametophytes of brown algae exerted by sediments. *Bulletin of the Japanese Society for Scientific Fisheries* 58: 619625
- Bell, T.W.; Allen, J.G.; Cavanaugh, K.C.; Siegel, D.A. (2020). Three decades of variability in California's giant kelp forests from the Landsat satellites. *Remote Sensing of the Environment* 238:110811. doi: 10.1016/j.rse.2018.06.039
- Bennett, S.; Wernberg, T.; Connell, S.D.; Hobday, A.J.; Johnson, C.R.; Poloczanska, E.S. (2015). The 'Great Southern Reef': social, ecological and economic value of Australia's neglected kelp forests. *Marine and Freshwater Research*, 67(1), 47–56. https://doi.org/10.1071/MF15232
- Blain, C.O.; Hansen, S.C.; Shears, N.T. (2021). Coastal darkening substantially limits the contribution of kelp to coastal carbon cycles. *Global Change Biology*, 27(21), 5547–5563. https://doi.org/10.1111/gcb.15837
- Blain, C.O.; Rees, T.A.V.; Hansen, C.S.; Shears, N.T. (2020). Morphology and photosynthetic response of the kelp *Ecklonia radiata* across a turbidity gradient. *Limnology and Oceanography*, 65(3), 529–544. https://doi.org/10.1002/lno.11321
- Butler, C.L.; Lucieer, V.L.; Wotherspoon, S.J.; Johnson, C.R. (2020). Multi-decadal decline in cover of giant kelp *Macrocystis pyrifera* at the southern limit of its Australian range. *Marine Ecology Progress Series* 653, 1–18. doi: 10.3354/meps13510
- Cavanaugh, K.C.; Reed, D.C.; Bell, T.W.; Castorani, M.C.; Beas-Luna, R. (2019). Spatial variability in the resistance and resilience of giant kelp in southern and Baja California to a multiyear heatwave. *Frontiers of Marine Science* 6:413. doi: 10.3389/fmars.2019.00413
- Cavanaugh, K.C.; Siegel, D.A.; Kinlan, B.P.; Reed, D.C. (2010). Scaling giant kelp field measurements to regional scales using satellite observations. *Marine Ecology Progress Series* 403, 13–27. doi: 10.3354/meps08467
- Cavanaugh, K.C.; Siegel, D.A.; Reed, D.C.; Dennison, P.E. (2011). Environmental controls of giant-kelp biomass in the Santa Barbara Channel, California. *Marine Ecology Progress Series* 429, 1–17. doi: 10.3354/meps09141

- Chapman, A.S.; Albrecht, A.S.; Fletcher, R.L. (2002). Differential effects of sediments on survival and growth of *Fucus serratus* embryos (fucales, phaeophyceae). *Journal of Phycology*, *38*(5), 894–903. https://doi.org/10.1046/j.1529-8817.2002.t01-1-02025.x
- Cheng, L.; von Schuckmann, K.; Abraham, J.P.; Trenberth, K.E.; Mann, M.E.; Zanna, L.; England, M.; Zika, J.; Fasullo, J.; Yu, Y.; Pan, Y.; Zhu, J.; Newsom, E.; Bronselaer, B.; Lin, X. (2022). Past and future ocean warming. *Nature Reviews Earth & Environment*, *3*(11), 776–794.
- Colombo-Pallotta, M.F.; García-Mendoza, E.; Ladah, L.B. (2006). Photosynthetic performance, light absorption, and pigment composition of *Macrocystis pyrifera* (laminariales, phaeophyceae) blades from different depths. *Journal of Phycology*, 42(6), 1225–1234. https://doi.org/10.1111/j.1529-8817.2006.00287.x
- Connell, S.D. (2005). Assembly and maintenance of subtidal habitat heterogeneity: synergistic effects of light penetration and sedimentation. *Marine Ecology Progress Series*, 289, 53–61.
- Connell, S.D.; Russell, B.D.; Turner, D.J.; Shepherd, S.A.; Kildea, T.; Miller, D.; Airoldi, L.; Cheshire, A. (2008). Recovering a lost baseline: missing kelp forests from a metropolitan coast. *Marine Ecology Progress Series*, 360, 63–72.
- Dean, T.A.; Jacobsen, F.R. (1986). Nutrient-limited growth of juvenile kelp, *Macrocystis pyrifera*, during the 1982Ü1984 "El Niño" in southern California. *Marine Biology* 90, 597–601. doi: 10.1007/BF00409280
- Desmond, M.J.; Pritchard, D.W.; Hepburn, C.D. (2015). Light limitation within southern New Zealand kelp forest communities. *PloS one*, *10*(4), e0123676.
- Devinny, J.S.; Volse, L.A. (1978). Effects of sediments on the development of *Macrocystis pyrifera* gametophytes. *Marine Biology*, 48(4), 343–348. https://doi.org/10.1007/BF00391638
- Doney, S.C.; Ruckelshaus, M.; Duffy, J.E.; Barry, J.P.; Chan, F.; English, C.A., Galindo, H.; Grebmeier, J.; Hollowed, A.; Knowlton, N.; Polovina, J.; Rabalais, N.; Sydeman, W.; Talley, L. (2011). Climate change impacts on marine ecosystems. *Annual Review of Marine Science* 4, 11–37.
- Edwards, M.; Hernandez-Carmona, G. (2005). Delayed recovery of giant kelp near its southern range limit in the North Pacific following El Niño. *Marine Biology* 147, 273–279.
- Eger, A.M.; Marzinelli, E.M.; Beas-Luna, R.; Blain, C.O.; Blamey, L.K.; Byrnes, J.E.K.; Carnell, P.E.; Choi, C.G.; Hessing-Lewis, M.; Kim, K.Y.; Kumagai, N.H.; Lorda, J.; Moore, P.; Nakamura, Y.; Pérez-Matus, A.; Pontier, O.; Smale, D.; Steinberg, P.D.; Vergés, A. (2023). The value of ecosystem services in global marine kelp forests. *Nature Communications*, *14*(1), 1894. https://doi.org/10.1038/s41467-023-37385-0
- Filbee-Dexter, K.; Scheibling, R.E. (2014). Sea urchin barrens as alternative stable states of collapsed kelp ecosystems. *Marine Ecology Progress Series*, 495, 1–25.
- Filbee-Dexter, K.; Wernberg, T. (2018). Rise of turfs: a new battlefront for globally declining kelp forests. *Bioscience*, 68(2), 64–76.
- Filbee-Dexter, K.; Wernberg, T.; Grace, S.P.; Thormar, J.; Fredriksen, S.; Narvaez, C.N.; Feehan, C.J.; Norderhaug, K.M. (2020). Marine heatwaves and the collapse of marginal North Atlantic kelp forests. *Scientific reports*, 10(1), p.13388.
- Foster, M.S.; Schiel, D.R. (1985). *The Ecology of Giant Kelp Forests in California: a Community Profile*. Washington, DC: US Fish and Wildlife Service.
- Foster, M. S., & Schiel, D. R. (2010). Loss of predators and the collapse of southern California kelp forests (?): alternatives, explanations and generalizations. *Journal of Experimental Marine Biology and Ecology*, 393(1–2), 59–70.

- Frölicher, T.L.; Fischer, E.M.; Gruber, N. (2018). Marine heatwaves under global warming. *Nature* 560, 360–364. doi: 10.1038/s41586-018-0383-9
- Gaitán-Espitia, J.D.; Hancock, J.R.; Padilla-Gamiño, J.L.; Rivest, E.B.; Blanchette, C.A.; Reed, D.C.; Hofmann, G.E. (2014). Interactive effects of elevated temperature and pCO2 on early-life-history stages of the giant kelp *Macrocystis pyrifera*. *Journal of Experimental Marine Biology and Ecology*, 457, 51–58.
- Gattuso, J.P.; Gentili, B.; Duarte, C.M.; Kleypas, J.A.; Middelburg, J.J.; Antoine, D. (2006). Light availability in the coastal ocean: impact on the distribution of benthic photosynthetic organisms and their contribution to primary production. *Biogeosciences*, 3(4), 489–513.
- Goff, J.R. (1997). A chronology of natural and anthropogenic influences on coastal sedimentation. *New Zealand Marine Geology* 138, 105–117. doi: 10.1016/s0025-3227(97)00018-2
- Gorgula, S.K.; Connell, S.D. (2004). Expansive covers of turf-forming algae on human-dominated coast: the relative effects of increasing nutrient and sediment loads. *Marine Biology*, 145(3), 613–619.
- Gupta, A.S.; Thomsen, M.; Benthuysen, J.A.; Hobday, A.J.; Oliver, E.; Alexander, L.V., et al. (2020). Drivers and impacts of the most extreme marine heatwaves events. *Sci. Rep.* 10, 1–15.
- Hamilton, S.L.; Bell, T.W.; Watson, J.R.; Grorud-Colvert, K.A.; Menge, B.A. (2020). Remote sensing: generation of long-term kelp bed data sets for evaluation of impacts of climatic variation. *Ecology* 101:e03031.
- Hay, C.H. (1990). The distribution of *Macrocystis* (Phaeophyta: Laminariales) as a biological indicator of cool sea surface temperature, with special reference to New Zealand waters. *Journal of the Royal Society of New Zealand* 20, 313–336. doi: 10.1080/03036758.1990.10426716
- Hepburn, C.D.; Holborow, J.D.; Wing, S.R.; Frew, R.D.; Hurd, C.L. (2007). Exposure to waves enhances the growth rate and nitrogen status of the giant kelp *Macrocystis pyrifera*. *Marine Ecology Progress Series* 339, 99–108. doi: 10.3354/meps339099
- Hernandez-Carmona, G.; Robledo, D.; Serviere-Zaragoza, E. (2001). Effect of nutrient availability on *Macrocystis pyrifera* recruitment and survival near its southern limit off Baja California. *Botanica Marina* 44, 221–229.
- Hobday, A.J.; Oliver, E.C.; Sen Gupta, A.S.; Benthuysen, J.A.; Burrows, M.T.; Donat, M.G., Holbrook, N.J.; Moore, P.J.; Thomsen, M.S.; Wernberg, T.; Smale, D.A. (2018). Categorizing and naming marine heatwaves. *Oceanography* 31, 162–173.
- Hoegh-Guldberg, O.; Bruno, J.F. (2010). The impact of climate change on the world's marine ecosystems. *Science* 328, 1523–1528.
- Huovinen, P.; Ramírez, J.; Palacios, M.; Gómez, I. (2020). Satellite-derived mapping of kelp distribution and water optics in the glacier impacted Yendegaia Fjord (Beagle Channel, Southern Chilean Patagonia). *Science of the Total Environment* 703:135531. doi: 10.1016/j.scitotenv.2019.135531
- Hynes, S.; Chen, W.; Vondolia, K.; Armstrong, C.; O'Connor, E. (2021). Valuing the ecosystem service benefits from kelp forest restoration: A choice experiment from Norway. *Ecological Economics*, 179, 106833. https://doi.org/10.1016/j.ecolecon.2020.106833
- Jack, L.; Wing, S.R. (2011). Individual variability in trophic position and diet of a marine omnivore is linked to kelp bed habitat. *Marine Ecology Progress Series*, 443, 129–139. https://doi.org/10.3354/meps09468
- Jack, L.; Wing, S.R.; McLeod, R.J. (2009). Prey base shifts in red rock lobster *Jasus edwardsii* in response to habitat conversion in Fiordland marine reserves: implications for effective spatial management. *Marine Ecology Progress Series*, 381, 213–222. https://doi.org/10.3354/meps07971

- Johansson, G.; Snoeijs, P. (2002). Macroalgal photosynthetic responses to light in relation to thallus morphology and depth zonation. *Marine Ecology Progress Series*, 244, 63–72. https://doi.org/10.3354/meps244063
- Kautsky, N.; Kautsky, H.; Kautsky, U.; Waern, M. (1986). Decreased depth penetration of *Fucus vesicolosus* (L.) since the 1940's indicates eutrophication of the Baltic Sea. *Marine Ecology Progress Series*, 28, 1–8.
- Kim, S.K.; Bhatnagar, I. (2011). Physical, chemical, and biological properties of wonder kelp-Laminaria. *Advances in Food and Nutrition Research*, 64, 85–96. https://doi.org/10.1016/b978-0-12-387669-0.00007-7
- Kirkman, H. (1989). Growth, density and biomass of *Ecklonia radiata* at different depths and growth under artifical shading off Perth, Western Australia. *Marine and Freshwater Research*, 40(2), 169–177.
- Kolodzey, S.; Stroh, A.K.; Wing, S.R. (2023). Small-scale differences in blue cod length distribution, growth, and trophic ecology in New Zealand. *Marine Ecology Progress Series*, 708, 125–142. https://doi.org/10.3354/meps14275
- Krumhansl, K.A.; Okamoto, D.K.; Rassweiler, A.; Novak, M.; Bolton, J.J.; Cavanaugh, K.C.; et al. (2016). Global patterns of kelp forest change over the past half-century. *Proceedings of the National Academy of Sciences*, 113(48), 13785–13790.
- Lee, Z.; Carder, K.L.; Arnone, R.A. (2002). Deriving inherent optical properties from water color: a multiband quasi-analytical algorithm for optically deep waters. *Applied Optics* 41, 5755–5772. doi: 10.1364/ao.41.005755
- Lee, Z.; Lubac, B.; Werdell, J.; Arnone, R. (2009). An update of the quasi-analytical algorithm (QAA_v5), in *International Ocean Color Group Software Report* (Dartmouth, NS: International Ocean Colour Coordinating Group), 1–9.
- Lee, Z.P.; Rhea, W.J.; Arnone, R.; Goode, W. (2005). Absorption coefficients of marine waters: Expanding multiband information to hyperspectral data. *IEEE Transactions on Geoscience and Remote Sensing* 43, 118–124. doi: 10.1109/tgrs.2004.839815
- Ling, S.D.; Johnson, C.R.; Frusher, S.D.; Ridgway, K. (2009). Overfishing reduces resilience of kelp beds to climate-driven catastrophic phase shift. *Proceedings of the National Academy of Sciences*, 106(52), 22341–22345.
- Ling, S.D.; Scheibling, R.E.; Rassweiler, A.; Johnson, C.R.; Shears, N.; Connell, S.D.; Salomon A.K.; Norderhaug, K.M.; Pérez-Matus, A.; Hernández, J.C.; Clemente, S.; Blamey, L.K.; Hereu, B.; Ballesteros, E.; Sala, E.; Garrabou, J.; Cebrian, E.; Zabala, M.; Fujita, D.; Johnson, L.E. (2015). Global regime shift dynamics of catastrophic sea urchin overgrazing. *Philosophical Transactions of the Royal Society B Biological Sciences*. 370:20130269. doi: 10.1098/rstb.2013.0269
- Mabin, C.J.; Johnson, C.R.; Wright, J.T. (2019). Physiological response to temperature, light, and nitrates in the giant kelp *Macrocystis pyrifera* from Tasmania, Australia. *Marine Ecology Progress Series* 614, 1–19. doi: 10.3354/meps12900
- Mak, W.; Hamid, N.; Liu, T.; Lu, J.; White, W.L. (2013). Fucoidan from New Zealand *Undaria* pinnatifida: monthly variations and determination of antioxidant activities. *Carbohydrate* Polymers, 95(1), 606–614. https://doi.org/10.1016/j.carbpol.2013.02.047
- Mangan, S.; Tait, L.W.; Wing, S.R.; D'Archino, R.; Neill, K.F.; Battershill, C.N.; Schiel, D.R. (2025). The relationships between macroalgae and New Zealand's wild fisheries, key vulnerabilities and monitoring approaches. *New Zealand Aquatic Environment and Biodiversity Report No.* 362. 40 p.
- Mangialajo, L.; Chiantore, M.; Cattaneo-Vietti, R. (2008). Loss of fucoid algae along a gradient of urbanisation, and structure of benthic assemblages. *Marine Ecology Progress Series*, 358, 63–74.

- McPherson, M.L.; Finger, D.J.; Houskeeper, H.F.; Bell, T.W.; Carr, M.H.; Rogers-Bennett, L. (2021). Large-scale shift in the structure of a kelp forest ecosystem co-occurs with an epizootic and marine heatwave. *Communications Biology* 4, 1–9. doi: 10.3354/meps11193
- Miller, R.J.; Lafferty, K.D.; Lamy, T.; Kui, L.; Rassweiler, A.; Reed, D.C. (2018). Giant kelp, *Macrocystis pyrifera*, increases faunal diversity through physical engineering. *Proceedings of the Royal Society B Biological Sciences* 285:20172571. doi: 10.1098/rspb.2017.2571
- Mora-Soto, A.; Palacios, M.; Macaya, E.C.; Gómez, I.; Huovinen, P.; Pérez-Matus, A.; Young, M.; Golding, N.; Toro, M.; Yaqub, M.; Macias-Fauria, M. (2020). A high-resolution global map of Giant kelp (*Macrocystis pyrifera*) forests and intertidal green algae (Ulvophyceae) with Sentinel-2 imagery. *Remote Sensing* 12:694. doi: 10.3390/rs12040694
- Morrison, M.A.; Lowe, M.L.; Parsons, D.M.; Usmar, N.R.; McLeod, I.M. (2009). A review of land-based effects on coastal fisheries and supporting biodiversity in New Zealand. *New Zealand Aquatic Environment and Biodiversity Report No. 37*. 100 p.
- Nelson, W.A. (2020). New Zealand Seaweeds: an Illustrated Guide. New Zealand: Te Papa Press.
- Nijland, W.; Reshitnyk, L.; Rubidge, E. (2019). Satellite remote sensing of canopy-forming kelp on a complex coastline: a novel procedure using the Landsat image archive. *Remote Sensing of Environment* 220, 41–50. doi: 10.1016/j.rse.2018.10.032
- Oliver, E.C.; Lago, V.; Hobday, A.J.; Holbrook, N.J.; Ling, S.D.; Mundy, C.N. (2018). Marine heatwaves off eastern Tasmania: trends, interannual variability, and predictability. *Progress in Oceanography* 161, 116–130. doi: 10.1016/j.pocean.2018.02.007
- Perkol-Finkel, S.; Airoldi, L. (2010). Loss and recovery potential of marine habitats: an experimental study of factors maintaining resilience in subtidal algal forests at the Adriatic Sea. *PLoS one*, 5(5), e10791.
- Pinkerton, M.; Gall, M.; Wood, S.; Zeldis, J. (2018). Measuring the effects of bivalve mariculture on water quality in northern New Zealand using 15 years of MODIS-Aqua satellite observations. *Aquaculture Environment Interactions* 10, 529–545. doi: 10.3354/aei00288
- Porse, H.; Rudolph, B. (2017). The seaweed hydrocolloid industry: 2016 updates, requirements, and outlook. *Journal of Applied Phycology*, 29(5), 2187–2200. https://doi.org/10.1007/s10811-017-1144-0
- Reed, D.C.; Rassweiler, A.; Carr, M.H.; Cavanaugh, K.C.; Malone, D.P.; Siegel, D.A. (2011). Wave disturbance overwhelms top-down and bottom-up control of primary production in California kelp forests. *Ecology*, *92*(11), 2108–2116.
- Reed, D.; Washburn, L.; Rassweiler, A.; Miller, R.; Bell, T.; Harrer, S. (2016). Extreme warming challenges sentinel status of kelp forests as indicators of climate change. *Nature Communications* 7, 1–7.
- Reynolds, R.W.; Banzon, V.F. (2008). NOAA Optimum Interpolation 1/4 Degree Daily Sea Surface Temperature (OISST) Analysis, Version 2 in NOAA National Centers for Environmental Information (Washington, DC: NOAA), V5SQ8XB5. doi: 10.1175/jcli-d-21-0001.1
- Rogers-Bennett, L.; Catton, C. (2019). Marine heat wave and multiple stressors tip bull kelp forest to sea urchin barrens. *Scientific Reports* 9, 1–9. doi: 10.3354/meps10573
- Salinger, M.J.; Diamond, H.J.; Behrens, E.; Fernandez, D.; Fitzharris, B.B.; Herold, N.; Johnstone, P.; Kerckhoffs, H.; Mullan, A.; Parker, A.; Renwick, J.; Scofield, C.; Siano, A.; Smith, R.; South, P.; Sutton, P.J.; Teixeira, E.; Thomsen, M.; Trought, M.C.T. (2020). Unparalleled coupled ocean-atmosphere summer heatwaves in the New Zealand region: drivers, mechanisms and impacts. *Climatic Change* 162(2) 485–506.
- Salinger, M.J.; Renwick, J.; Behrens, E.; Mullan, A.B.; Diamond, H.J.; Sirguey, P.; Smith, R.O.; Trought, M.; Alexander, L.; Cullen, N.J.; Fitzharris, B.B.; Hepburn, C.D.; Parker, A.K.; Sutton, P.J. (2019). The unprecedented coupled ocean-atmosphere summer heatwave in the

- New Zealand region 2017/18: drivers, mechanisms and impacts. *Environmental Research Letters* 14:044023. doi: 10.1088/1748-9326/ab012a
- Schiel, D.R.; Foster, M.S. (2015). *The Biology and Ecology of Giant Kelp Forests*. California: Univ. of California Press.
- Schiel, D.R.; Gunn, T.D. (2019). Effects of sediment on early life history stages of habitat-dominating fucoid algae. *Journal of Experimental Marine Biology and Ecology* 516, 44–50. doi: 10.1016/j.jembe.2019.04.005
- Schiel, D. R.; Nelson, W. A. (1990). The harvesting of macroalgae in New Zealand. *Hydrobiologia*, 204, 25-33
- Schiel, D.R.; Wood, S.A.; Dunmore, R.A.; Taylor, D.I. (2006). Sediment on rocky intertidal reefs: Effects on early post-settlement stages of habitat-forming seaweeds. *Journal of Experimental Marine Biology and Ecology*, 331(2), 158–172. https://doi.org/10.1016/j.jembe.2005.10.015
- Schlieman, C.D.; Wing, S.R.; O'Connell-Milne, S.A.; McMullin, R.M.; Durante, L.M.; Kolodzey, S.; Frew, R.D. (2022). Catchment modifications influence the composition of basal organic matter supporting suspension-feeding bivalves. *Estuarine, Coastal and Shelf Science*, 275, 107989. https://doi.org/10.1016/j.ecss.2022.107989
- Seymour, R.J.; Tegner, M.J.; Dayton, P.K.; Parnell, P.E. (1989). Storm wave induced mortality of giant kelp, *Macrocystis pyrifera*, in southern California. *Estuarine, Coastal and Shelf Science*, 28(3), 277–292.
- Shears, N.T.; Babcock, R.C. (2002). Marine reserves demonstrate top-down control of community structure on temperate reefs. *Oecologia*, 132(1), 131–142.
- Shears, N.T.; Babcock, R.C.; Salomon, A.K. (2008). Context-dependent effects of fishing: Variation in trophic cascades across environmental gradients. *Ecological Applications*, 18(8), 1860–1873.
- Shi, W.; Wang, M. (2007). Detection of turbid waters and absorbing aerosols for the MODIS ocean color data processing. *Remote Sensing of the Environment* 110, 149–161. doi: 10.1016/j.rse.2007.02.013
- Smale, D.A. (2020). Impacts of ocean warming on kelp forest ecosystems. *New Phytologist* 225, 1447–1454. doi: 10.1111/nph.16107
- Smale, D.A.; Wernberg, T. (2013). Extreme climatic event drives range contraction of a habitat-forming species. *Proceedings of the Royal Society B: Biological Sciences*, 280(1754), p.20122829.
- Smale, D.A.; Wernberg, T.; Oliver, E.C.; Thomsen, M.; Harvey, B.P.; Straub, S.C.; Burrows, M.; Alexander, L.; Benthuysen, J.; Donat, M.; Feng, M.; Hobday, A.; Holbrook, N.; Perkins-Kirkpatrick, S.; Scannell, H.; Sen Gupta, A.; Payne, B.; Moore, P. (2019). Marine heatwaves threaten global biodiversity and the provision of ecosystem services. *Nature Climate Change* 9, 306–312. doi: 10.1038/s41558-019-0412-1
- Steneck, R.S.; Graham, M.H.; Bourque, B. J.; Corbett, D.; Erlandson, J.M.; Estes, J.A.; Tegner, M.J. (2002). Kelp forest ecosystems: biodiversity, stability, resilience and future. *Environmental conservation*, 29(4), 436–459.
- Straub, S.C.; Wernberg, T.; Thomsen, M.S.; Moore, P.J.; Burrows, M.; Harvey, B.P.; Smale, D.A. (2019). Resistance to obliteration; responses of seaweeds to marine heatwaves. *Frontiers of Marine Science* 6:763. doi: 10.3389/fmars.2019.00763
- Tait, L.W. (2014). Impacts of natural and manipulated variations in temperature, pH and light on photosynthetic parameters of coralline–kelp assemblages. *Journal of Experimental Marine Biology and Ecology* 454, 1–8. doi: 10.1016/j.jembe.2014.01.016

- Tait, L.W. (2019). Giant kelp forests at critical light thresholds show compromised ecological resilience to environmental and biological drivers. *Estuarine, Coastal and Shelf Science* 219, 231–241. doi: 10.1016/j.ecss.2019.02.026
- Tait, L.W.; Thoral, F.; Pinkerton, M.H.; Thomsen, M.S.; Schiel, D.R. (2021). Loss of giant kelp, *Macrocystis pyrifera*, driven by marine heatwaves and exacerbated by poor water clarity in New Zealand. *Frontiers in Marine Science*, 8, 721087.
- Taylor, D.I.; Schiel, D.R. (2003). Wave-related mortality in zygotes of habitat-forming algae from different exposures in southern New Zealand: the importance of 'stickability'. *Journal of Experimental Marine Biology and Ecology* 290, 229–245. doi: 10.1016/s0022-0981(03)00094-7
- Tegner, M.J.; Dayton, P.K. (2000). Ecosystem effects of fishing in kelp forest communities. *ICES Journal of Marine Science*, 57(3), 579–589.
- Thomsen, M.S.; Mondardini, L.; Alestra, T.; Gerrity, S.; Tait, L.; South, P.M.; Lilley, S.A.; Schiel, D.R. (2019). Local extinction of bull kelp (Durvillaea spp.) due to a marine heatwave. *Frontiers in Marine Science* 6:84. doi: 10.3389/fmars.2019.00084
- Vásquez, J.A.; Zuñiga, S.; Tala, F.; Piaget, N.; Rodríguez, D.C.; Vega, J.M.A. (2014). Economic valuation of kelp forests in northern Chile: values of goods and services of the ecosystem. *Journal of Applied Phycology*, 26(2), 1081–1088. https://doi.org/10.1007/s10811-013-0173-6
- Wernberg, T.; Bennett, S.; Babcock, R.C.; De Bettignies, T.; Cure, K.; Depczynski, M.; et al. (2016). Climate-driven regime shift of a temperate marine ecosystem. *Science*, 353(6295), 169–172.
- Wernberg, T.; Smale, D.A.; Tuya, F.; Thomsen, M.S.; Langlois, T.J.; De Bettignies, T.; Bennett, S.; Rousseaux, C. (2013). An extreme climatic event alters marine ecosystem structure in a global biodiversity hotspot. *Nature Climate Change* 3, 78–82. doi: 10.1038/nclimate1627
- Wernberg, T.; Thomsen, M.S.; Tuya, F.; Kendrick, G.A.; Staehr, P.A.; Toohey, B.D. (2010). Decreasing resilience of kelp beds along a latitudinal temperature gradient: potential implications for a warmer future. *Ecological Letters* 13, 685–694. doi: 10.1111/j.1461-0248.2010.01466.x
- White, L.; White, W.L. (2020). Seaweed utilisation in New Zealand. *Botanica Marina*, *63*(4), 303–313. https://doi.org/10.1515/bot-2019-0089
- Wing, S.; Jack, L. (2012). Resource specialisation among suspension-feeding invertebrates on rock walls in Fiordland, New Zealand, is driven by water column structure and feeding mode. *Marine Ecology Progress Series*, 452, 109–118. https://doi.org/10.3354/meps09588
- Wing, S.R.; Beer, N.A.; Jack, L. (2012). Resource base of blue cod *Parapercis colias* subpopulations in marginal fjordic habitats is linked to chemoautotrophic production. *Marine Ecology Progress Series*, 466, 205–214. https://doi.org/10.3354/meps09929
- Wing, S.R.; Shears, N.T.; Tait, L.W.; Schiel, D.R. (2022). The legacies of land clearance and trophic downgrading accumulate to affect structure and function of kelp forests. *Ecosphere*, *13*(12), e4303.